

# Haloalkane Dehalogenases From Marine Organisms

Antonin Kunka<sup>\*,†</sup>, Jiri Damborsky<sup>\*,†</sup>, Zbynek Prokop<sup>\*,†,1</sup>

<sup>\*</sup>Loschmidt Laboratories, Department of Experimental Biology, Research Centre for Toxic Compounds in the Environment RECETOX, Faculty of Science, Masaryk University, Brno, Czech Republic

<sup>†</sup>International Clinical for Research Center, St. Anne's University Hospital, Brno, Czech Republic

<sup>1</sup>Corresponding author: e-mail address: zbynek@chemi.muni.cz

## Contents

1. Introduction	2
2. Identification of HLDs From Marine Organisms	3
2.1 HLDs From Pollution-Degrading Microorganisms	4
2.2 HLDs From Symbiotic Microorganisms	4
2.3 HLDs From Genomic Databases	5
2.4 HLDs From Metagenomic Libraries	6
3. Characteristics of Marine HLDs	7
3.1 Specific Activity	7
3.2 Steady-State Kinetics	11
3.3 Enantioselectivity	13
3.4 Structure and Stability	13
4. Experimental Characterization of HLDs	17
4.1 Expression and Purification	17
4.2 Specific Activity	18
4.3 Steady-State Kinetics	26
4.4 Enantioselectivity	32
4.5 Stability	33
5. Conclusions and Perspectives	37
Acknowledgments	39
References	39

## Abstract

Haloalkane dehalogenases degrade halogenated compounds to corresponding alcohols by a hydrolytic mechanism. These enzymes are being intensively investigated as model systems in experimental and in silico studies of enzyme mechanism and evolution, but also hold importance as useful biocatalysts for a number of biotechnological applications. Haloalkane dehalogenases originate from various organisms including bacteria (degraders, symbionts, or pathogens), eukaryotes, and archaea. Several members of this enzyme family have been found in marine organisms. The marine environment represents a good source of enzymes with novel properties, because of its diverse

living conditions. A number of novel dehalogenases isolated from marine environments show interesting characteristics such as high activity, unusually broad substrate specificity, stability, or selectivity. In this chapter, the overview of haloalkane dehalogenases from marine organisms is presented and their characteristics are summarized together with an overview of the methods for their identification and biochemical characterization.



## 1. INTRODUCTION

Haloalkane dehalogenases (EC 3.8.1.5, HLDs) belong to the large group of structurally similar hydrolases that share common  $\alpha/\beta$  hydrolase fold with lipases, esterases, carboxypeptidases, and acetylcholinesterases (Nardini & Dijkstra, 1999; Ollis et al., 1992). HLDs are globular proteins consisting of the conserved main domain and flexible cap domain with active site buried at their interface and connected to protein surface by access tunnels (Damborsky, Chaloupkova, Pavlova, Chovancova, & Brezovsky, 2010). HLDs catalyze the conversion of chlorinated, brominated, and iodinated aliphatic compounds containing monohalogenated  $sp^3$ -hybridized carbon, to corresponding alcohol, halide, and proton (Damborsky et al., 2001). Based on a phylogenetic analysis, HLDs can be divided into three groups, denoted as HLD-I, HLD-II, and HLD-III (Chovancova, Kosinski, Bujnicki, & Damborsky, 2007). A considerable amount of information on the structural, mechanistic, and kinetic level is known about the members of HLD-I and HLD-II groups, in contrast with proteins from subfamily HLD-III for which the tertiary structure is not available.

First HLDs were isolated from soil-growing bacteria (Keuning, Janssen, & Witholt, 1985; Kulakova, Larkin, & Kulakov, 1997; Nagata et al., 1993), but later have been found in symbiotic (Sato et al., 2005), marine (Hesseler et al., 2011), or pathogenic bacteria (Hasan et al., 2011), archaea (Vanacek et al., 2018), and eukaryotic organisms (Fortova et al., 2013). Genes encoding HLDs are found in catabolic clusters of xenobiotic compounds in organohalogen-degrading bacteria (Nagata, Miyauchi, & Takagi, 1999; Poelarends et al., 2000) that are often associated with transposable elements and insertion sequences (Janssen, Dinkla, Poelarends, & Terpstra, 2005; Poelarends, Kulakov, Larkin, Van Hylckama Vlieg, & Janssen, 2000). However, biological function in other organisms, evolutionary origins, and natural substrates are still unknown.

Due to their catalytic properties and broad substrate specificity, HLDs have found utilization in bioremediation of groundwaters (Dvorak, Bidmanova,

Damborsky, & Prokop, 2014; Stucki & Thüer, 1995), decontamination of warfare agents (Prokop, Oplustil, DeFrank, & Damborsky, 2006), preparation of optically pure building blocks for organic synthesis (Chaloupkova, Prokop, Sato, Nagata, & Damborsky, 2011; Hasan et al., 2011; Prokop et al., 2010; Westerbeek et al., 2011), biosensing of environmental pollutants (Bidmanova, Chaloupkova, Damborsky, & Prokop, 2010; Bidmanova, Damborsky, & Prokop, 2013; Campbell, Müller, & Reardon, 2006), or protein tagging for cell imaging and protein analysis (Ohana et al., 2009).

Structural and biochemical characterization and detailed analysis of novel members of HLD family are crucial for the understanding of their structure–function relationships. Feature comparisons of HLDs from organisms living in diverse habitats allow analysis of their biological function and evolutionary origins. The marine environment accommodates organisms from all living phyla that have their molecular machinery adapted to extraordinary living conditions such as extreme pressures and temperatures, a high concentration of salts, and limited or no access to oxygen and light. Proteins isolated from such environment display interesting properties. Several members of HLD family have been found in genomes of marine organisms and show interesting properties such as high activity, enantioselectivity, stability, and broad substrate specificity (Fortova et al., 2013; Gehret et al., 2012; Hesseler et al., 2011; Jesenska et al., 2009; Li & Shao, 2014; Novak et al., 2014; Tratsiak et al., 2013). Here, the overview of HLDs from marine organisms is presented together with methods for their identification and experimental characterization.



## 2. IDENTIFICATION OF HLDs FROM MARINE ORGANISMS

Since the identification of the first HLD 33 years ago (Keuning et al., 1985), 33 novel HLDs have been described and biochemically characterized. The fact that 40% of new HLDs were found in marine organisms during the last 8 years suggests the enormous potential of the marine environment as a pool of genetic diversity. The biological role and evolutionary origins of HLDs remain elusive, and although some working hypotheses have been proposed, the discovery of novel variants and their characterization is needed to provide experimental evidence. The following section gives an overview of novel HLDs from marine organisms and approaches that have been used for their identification.

## 2.1 HLDs From Pollution-Degrading Microorganisms

Oil spills and industrial waste are the major sources of ocean and sea pollution and represent an enormous threat to marine organisms. Biodegradation of anthropogenic compounds is carried out mostly by bacteria capable of utilizing these substances as a sole source of carbon and energy via a specialized enzymatic pathway. *Alcanivorax* bacteria cannot utilize carbohydrates and amino acids for their growth (Yakimov et al., 1998), but produce biosurfactants when grown on n-alkanes (Abraham, Meyer, & Yakimov, 1998). These bacteria become predominant in crude oil-containing waters when nitrogen and phosphorus are supplied (Kasai et al., 2002).

Analyses of a metabolic pathway for long-chain alkane degradation in *Alcanivorax dieselolei* B-5 (Liu & Shao, 2005) isolated from the oil-contaminated surface water of Bohai sea revealed the important role of alkane hydroxylases (Liu et al., 2011; Wang & Shao, 2014). The degrading activity of *A. dieselolei* B-5 toward 1-chlorohexadecane was discovered in the surface waters of the Arctic sea, and HLD-coding gene, *dadB*, was subsequently identified (Li & Shao, 2014). Following protein expression and biochemical characterization revealed that this enzyme possesses one of the highest overall activities toward halogenated substrates of all previously characterized HLDs to date, which makes it a suitable target for future protein engineering studies.

## 2.2 HLDs From Symbiotic Microorganisms

Apart from the anthropogenic origin, large numbers of organohalogen compounds with interesting chemistry (peptides, polyketides, indoles, terpenes, phenols, etc.) are produced by marine algae, bacteria, sponges, gorgonians, bryophytes, cyanobacteria, fungi, and marine invertebrates (Agarwal et al., 2017; Ahn et al., 2003; Gribble, 2015; Van Pee, 2001). These halogenated organic compounds show a wide variety of biological activities: antibacterial, antifungal, antiparasitic, antitumor, antiviral, antiinflammatory, or antioxidant and thus have a great biotechnological value (Gribble, 2015; Van Pee & Unversucht, 2003).

Although a large number of marine halometabolites have been identified, rather little is known about their biological function. It was suggested that they play a role in the chemical defense of marine organisms and function as an antifouling agent against consumers and pathogens (Ahn et al., 2003; Cabrita, Vale, & Rauter, 2010; König & Wright, 1997; Lane et al., 2009). Recently, different signaling roles of halogenated compound tetrabromopyrrole between bacteria and corals were described, suggesting a potential role of

halogenated compounds in interspecies communication (Sneed, Sharp, Ritchie, & Paul, 2014).

The microorganisms living in a symbiosis with organohalogen-producing organisms may use dehalogenase enzymes to degrade some of the toxic compounds. Recently, dehalogenase activity was confirmed in members of *Rhodobacteraceae* family isolated from the surface of marine sponge *Hymeniacidon perlevis* (Huang, Xin, Cao, & Zhang, 2011). Subsequently, genes encoding L-haloacid dehalogenase DehRh<sub>b</sub> and haloalkane dehalogenase HanR have been isolated, cloned, and overexpressed in *Escherichia coli* (Novak et al., 2014, 2013).

### 2.3 HLDs From Genomic Databases

Recent rapid development of sequencing technologies and high-throughput screening assays enabled us to access the genetic information of marine microorganisms without cultivation. Novel enzymes catalyzing a wide range of reactions were identified in marine microbial biomass isolated from different marine habitats by a combination of proteomic and genomic analysis (Hårdeman & Sjöling, 2007; Hu et al., 2010; Kennedy, Marchesi, & Dobson, 2008). The gene coding HLD DmmA, originally annotated as CurN (Chang et al., 2004), was identified in the cosmid library developed from the field isolate *Moorea producens* (Engene et al., 2012). Originally, DmmA was presumed to be a final gene product of the curacin A biosynthetic gene cluster of this marine cyanobacterium. However, attempts to amplify the gene from *M. producens* genome were unsuccessful and the origin of *dmmA* gene remains unknown. It is speculated that the origin may be symbiont or associated bacterium and the natural function of DmmA is to dehalogenase molecules produced by *M. producens* (Gehret et al., 2012).

Next-generation sequencing technologies enable rapid collection of genome sequences that represent a gold mine for the discovery of novel proteins. The number of sequences deposited to GenBank database surpassed 200 million in April 2017 (Clark, Karsch-Mizrachi, Lipman, Ostell, & Sayers, 2016). Mining of metagenome and genome databases has proven an invaluable method for the discovery of novel nitrilases (Gong et al., 2013), halohydrin dehalogenases (Koopmeiners, Halmschlag, Schallmeyer, & Schallmeyer, 2016; Schallmeyer, Koopmeiners, Wells, Wardenga, & Schallmeyer, 2014), transaminases (Guo & Berglund, 2017), and endoglucanases (Qiu et al., 2011). Of special interest are enzymes from microorganisms which thrive in extreme environments and have their metabolic function and molecular machinery adapted to their natural habitat.

The genes coding for HLDs were identified in the genome of marine organisms: *dhcA* from halophilic  $\gamma$ -proteobacteria *Hahella chejuensis* KCTC 2396 (Lee et al., 2001), *drbA* from aerobic and heterotrophic member of Planctomycetales order *Rhodopirellula baltica* SH1 (Glockner et al., 2003; Jesenska et al., 2009), *dppA* from myxobacterium *Plesiocystis pacifica* SIR-1 (Hesseler et al., 2011; Iizuka et al., 2003), *dmxA* from psychrophilic *Marinobacter* sp. ELB17 (Tratsiak et al., 2013), and *dspA* from sea urchin *Strongylocentrotus purpuratus*, which is the first HLD of eukaryotic origin (Fortova et al., 2013). Moreover, four genes of novel HLDs from the extreme environment, *dmsaA* from halophile *Marinobacter santoriniensis* NKSG1, *dpaA* and *dpaB* from psychrophilic halophile *Paraglaciecola agarilytica* NO2, and *dpgA* from psychrophilic  $\gamma$ -proteobacterium NOR5-3, have been identified and characterized using a combination of bioinformatics tools and automated laboratory screening techniques (Vanacek et al., 2018).

## 2.4 HLDs From Metagenomic Libraries

The marine environment represents a perfect target for the search of novel enzymes, because of the diverse living conditions that various organisms can inhabit. For example, mining of metagenomic libraries from extreme habitats led to the discovery of novel esterases with no significant amino acid sequence similarity to any currently known esterases (Ferrer, Belouqui, Timmis, & Golyshin, 2008). Metagenomics has emerged as a useful technology that overcomes a difficulty with a very low percentage of cultivatable marine microorganisms. This approach has recently been successfully used for identification of two novel HLDs in samples from groundwater in industrial areas (Kotik, Vanacek, Kunka, Prokop, & Damborsky, 2017). Such results support the idea of its use for identification of HLDs in marine sediments, polluted water areas, or microbial consortia associated with marine sponges or coral reefs, with a high occurrence of natural organohalogen compounds.

Despite indisputable advances in the field, there are still many challenges that need to be overcome. Development of high-throughput screening methods and synthesis of chromogenic or fluorogenic substrates for the detection of enzymes are a necessity to increase a success rate of function-based metagenomic screens. Novel lab-on-a-chip technologies can significantly accelerate such a functional screening which is significantly lagging behind sequencing. Moreover, the large amount of data generated by metagenomics and other sequencing projects needs to be deposited in knowledge bases with proper annotation. Automated and robust bioinformatics pipelines need to be developed to extract the relevant information from these databases (DeCastro, Rodríguez-Belmonte, & González-Siso, 2016).



### 3. CHARACTERISTICS OF MARINE HLDs

HLD enzymes identified in the marine environment have been subjected to extensive biochemical and biophysical characterization (Table 1). Their properties, including specific activity, kinetic parameters, enantioselectivity, and stability, will be discussed in this section.

#### 3.1 Specific Activity

Marine HLDs show a broad range of substrate specificities similar to other characterized HLDs (Table 1). The overall activity of marine HLDs with the set of 30 halogenated substrates (Table 2) ranges between 0.1 and 400 nmols<sup>-1</sup> mg<sup>-1</sup> of protein with preference for brominated and iodinated substrates over the chlorinated compounds. Additionally, the activity of DmmA, DppA, and DadB was assayed and detected toward halogenated compounds outside the panel of most commonly tested substrates (Burycka et al., 2018; Daniel, Burycka, Prokop, Damborsky, & Brezovsky, 2014; Hesseler et al., 2011; Li et al., 2014).

High specific activity has been recently reported for DadB from *A. dieselolei* B-5 (Li et al., 2014). DadB shows broad substrate specificity and can degrade all 30 representative substrates (Table 2) except for chlorocyclohexane. It prefers short (C<sub>2</sub>–C<sub>3</sub>) and brominated substrates over their iodinated and chlorinated counterparts, but can convert even compounds with longer chain lengths (C<sub>4</sub>–C<sub>14</sub>). The activity of DadB with iodinated substrates is lower than DbjA and LinB, while its activity toward brominated substrates is generally higher than for five other representative members of HLD group—DhaA, LinB, DhlA, DbjA, and DmbA (Li et al., 2014).

Unusually broad substrate specificity has been reported for DmmA (Burycka et al., 2018). DmmA converts all but 1 of the 30 typical substrates. DmmA is the only enzyme that can convert all poorly degradable chlorinated environmental pollutants, 1,2-dichloroethane, 1,2-dichloropropane, 1,2,3-trichloropropane, chlorocyclohexane, and (bromomethyl)cyclohexane. Moreover, it is active toward newly identified halogenated substrates with novel structural motives (Burycka et al., 2018; Daniel et al., 2014) and can catalyze the complete conversion of 1,2-dibromoethane and 1,2,3-tribromopropane to ethylene glycol and glycerol, respectively. These features make DmmA a promising enzyme for various applications in the field of biodegradation (Burycka et al., 2018).

**Table 1** Overview of HLDs From Marine Organisms and Their Biochemical Properties

	DadB	DppA	HanR	DrbA	DmmA	DspA	DmxA	DhcA	DmsaA	DgpA	DpaA	DpaB
<i>Occurrence</i>												
Source organism	<i>Alcanivorax dieselolei</i> B-5	<i>Plesiocystis pacifica</i> SIR-1	<i>Rhodobacteraceae</i> species	<i>Rhodopirellula baltica</i> SH1	Unknown	<i>Strongylocentrotus purpuratus</i>	<i>Marinobacter</i> sp. ELB17	<i>Hahella chejuensis</i> KCTC 2396	<i>Marinobacter santoriniensis</i> NKSG1	<i>γ-Proteobacterium</i> NOR5-3	<i>Paraglacicola agarilytica</i> NO2	<i>Paraglacicola agarilytica</i> NO2
<i>Evolution</i>												
Subfamily	II	I	II	III	II	II	II	III	I	I	I	I
<i>Catalytic efficiency</i>												
$K_m$ range (mM)	0.8–15.1	0.8–45.2		0.06	0.4–2.3	0.9	0.03–0.8		1.75	1.61	3.7	1.49
$k_{cat}$ range ( $s^{-1}$ )	1.2–34.3	0.4–9.9		0.13	0.2–1.8	1.6	1.9–2.6		0.17	0.04	0.06	0.09
$k_{cat}/K_m$ range ( $s^{-1} mM^{-1}$ )	0.2–16.4	0.1–4.0		2	0.5–1.3	1.8	2.4–88.1		0.1	0.02	0.02	0.06
<i>Activity and specificity</i>												
Overall activity	***	*	*	*	*	*	*	*	**	*	*	**
Chlorinated substrates	**	x	**	*	*	*	**	x	*	*	*	*
Brominated substrates	***	***	**	*	*	*	**	***	**	**	**	**
Iodinated substrates	***			*	*	*	**	***	*	**	**	**
Poor substrates	**	x	*	x	***	*	*	*	*	*	*	*
<i>Enantioselectivity</i>												
$\alpha$ -Bromoesters					**	x	***		*	x	***	***
$\beta$ -Bromoalkanes					x	*	*		x	x	*	x



<i>Stability</i>												
Predicted pI	5.2	4.9	4.9	7.1	5.4	6.4	5.5	6.1	6.5	4.6	4.6	5.2
pH profile maximum	8	8–9		9.2	8.7		7–9			8.9	8	8.8
Temp. profile maximum (°C)	50	30–37		50	40		55			25	25	25
Apparent melting temp. (°C)				39.4	49.1	44.2	65.9	54.6	51.4	36.6	38.2	37.3
<i>Structural information</i>												
Predicted $M_w$ (kDa)	33.2	32.5	32.8	36.3	33.3	35.5	34.1	34.8	33.6	37.2	34.3	33.7
Units in quaternary structure	1	1	1	∞	1, 2	1, 2	1, 2	∞	∞	1	2	1
<i>References</i>												
Original publication	Li et al. (2014)	Hesseler et al. (2011)	Novak et al. (2014)	Jesenska et al. (2009)	Gehret et al. (2012) and Buryska, Babkova, Vavra, Damborsky, and Prokop (2018)	Fortova et al. (2013)	Tratsiak et al. (2013) and Chrast et al. (2018)	Unpublished data		Vanacek et al. (2018)		

*Asterisks* depict qualitative measure of activity or enantioselectivity (the higher number refers to higher activity/selectivity), x—not active or nonselective, empty field—data not available, ∞—high-order multimeric structure. Overall activity was estimated from the specific activities toward 30 selected substrates (Koudelakova et al., 2011) with the exception of HanR, for which only a semiquantitative evaluation was done based on the available data. Poor substrates were selected based on the authors' review (Koudelakova et al., 2011). The isoelectric points (pI) and molecular weights ( $M_w$ ) were predicted from the sequence using ExPASy server (Gasteiger et al., 2003). Apparent melting temperatures were determined from circular dichroism data as the midpoints of temperature transitions.

**Table 2** Physicochemical Properties of 30 Halogenated Substrates Selected for Determination of Substrate Specificity Profiles

No.	Substrate	$M_w$ (g/mol)	Vapor Pressure (kPa)	Solubility (mM)	Log <i>P</i> (Octanol/ Water)
1	1-Chlorobutane	93	33.66	11.9	2.6
2	1-Chlorohexane	121	1.25	0.8	3.6
3	1-Bromobutane	137	5.60	6.3	2.7
4	1-Bromohexane	165	0.52	0.2	3.8
5	1-Iodopropane	170	5.75	6.3 <sup>(20°C)</sup>	2.6
6	1-Iodobutane	184	1.85	1.1 <sup>(20°C)</sup>	3.1
7	1-Iodohexane	212	0.19	0.1*	4.2
8	1,2-Dichloroethane	99	26.29	86.9	1.5
9	1,3-Dichloropropane	113	2.43	24.3	2.0
10	1,5-Dichloropentane	141	0.16	0.9	2.8
11	1,2-Dibromoethane	188	1.60	20.8	2.1
12	1,3-Dibromopropane	202	0.18	8.4 <sup>(20°C)</sup>	2.6
13	1-Bromo-3-chloropropane	157	0.85	14.2	2.2
14	1,3-Diiodopropane	296	0.06*	0.1*	3.0
15	2-Iodobutane	184	2.28	1.1 <sup>(18°C)</sup>	2.9
16	1,2-Dichloropropane	113	17.76	24.8	2.0
17	1,2-Dibromopropane	202	1.05	7.1	2.4
18	2-Bromo-1-chloropropane	157	5.70*	14.2	2.0
19	1,2,3-Trichloropropane	147	0.40	11.9	2.0
20	Bis(2-chlorethyl)ether	109	3.61*	147.5*	1.1
21	Chlorocyclohexane	119	0.90	4.2	3.0
22	Bromocyclohexane	163	0.33*	5.1	3.2
23	1-(Bromomethyl)cyclohexane	177	0.18*	0.1*	3.7
24	1-Bromo-2-chloroethane	143	4.41	48.1	1.6
25	Chlorocyclopentane	105	2.72*	3.9*	2.5

**Table 2** Physicochemical Properties of 30 Halogenated Substrates Selected for Determination of Substrate Specificity Profiles—cont'd

No.	Substrate	$M_w$ (g/mol)	Vapor Pressure (kPa)	Solubility (mM)	Log $P$ (Octanol/ Water)
26	4-Bromobutyronitrile	148	0.04*	27.9*	0.9
27	1,2,3-Tribromopropane	281	0.02*	0.2*	3.3
28	1,2-Dibromo-3-chloropropane	236	0.08 <sup>(20°C)</sup>	5.2 <sup>(20°C)</sup>	2.7
29	3-Chloro-2-methylprop-1-ene	91	13.60 <sup>(20°C)</sup>	15.5	2.2
30	2,3-Dichloroprop-1-ene	111	8.16	19.4	2.2

Vapor pressure is related to the compound volatility (higher value means more volatile). Log  $P$  is a partition coefficient of the compound between water and octanol and quantifies polarity of compound (positive values—hydrophobic, negative values—hydrophilic). All the values were taken from ChemSpider (<http://www.chemspider.com/>). The values were measured at 25°C unless stated otherwise. Values denoted by the asterisk (\*) were estimated using Antoine and Grain equation or calculated from the partition coefficient for vapor pressure and solubility, respectively. The set of compounds was selected using the multivariate statistical design (Koudelakova et al., 2011).

DrbA from *R. baltica* SH1 (Jesenska et al., 2009) and Dhca from *H. chejuensis* KCTC 2396 (unpublished results) show very low activity toward the typical set of HLD substrates. They belong to the HLD-III subfamily that comprises of proteins having a unique catalytic pentad D-H-D + W-N (Chovancova et al., 2007). Enzymes from this group are produced in low amount, form large oligomeric structures, and display several orders of magnitude lower activity toward typical HLD substrates. No experimental structures of these enzymes are currently available.

### 3.2 Steady-State Kinetics

The catalytic efficiency of marine dehalogenases shows no significant deviation from other characterized HLDs (Kokkonen, Koudelakova, Chaloupkova, Prokop, & Damborsky, 2017). The Michaelis–Menten constant  $K_M$  for various halogenated substrates ranges between 0.03 and 45 mM (HLDs: 0.005–48 mM) and the catalytic constant  $k_{cat}$  is from 0.02 to 34 s<sup>−1</sup> (HLDs: 0.02–40 s<sup>−1</sup>).

DmxA from the psychrophilic bacterium *Marinobacter* sp. ELB17 displays the highest catalytic efficiency of all HLDs found in the marine environment with  $k_{cat}/K_M = 88.1 \text{ s}^{-1} \text{ mM}^{-1}$  with 1,3-dibromopropane (Chrast et al., 2018). The kinetic mechanism of DmxA with 1,3-dibromopropane is

complex and involves positive cooperativity and partial substrate inhibition. Interestingly, mutation of the unique halide-stabilizing Q40 to conventional N, which is typical for members of HLD-II group (Chovancova et al., 2007), resulted in the 12-times increased  $k_{\text{cat}}$ . Moreover, this mutation diminished the cooperativity of DmxA conversion of 1,3-dibromopropane and lowered the effect of substrate inhibition (Chrast et al., 2018).

The steady-state kinetics of DadB from *A. dieselolei* B-5 reflects its high specific activity. DadB has a low affinity (0.8–15 mM), but high catalytic constant around  $20\text{s}^{-1}$  on average for short brominated substrates (Li et al., 2014), with the highest catalytic efficiency toward 1,3-dibromopropane ( $k_{\text{cat}}/K_{\text{M}} = 16.4\text{s}^{-1}\text{mM}^{-1}$ ). Surprisingly, DadB prefers short brominated substrates which are not typical for other HLDs with a large active site and/or wide access tunnel. Due to its unusual properties, DadB represents a good model system for studying structure–function relationships of HLDs as well as a good target for protein engineering studies.

HLD DmmA isolated from marine consortium has widely opened access pathways and large active site cavity that most likely explains its broad substrate specificity, unique among the HLDs (Buryska et al., 2018). In contrast to DadB, it can bind and convert longer substrates, even though with low efficiency ( $k_{\text{cat}}/K_{\text{M}} = 0.45\text{--}1.3\text{s}^{-1}\text{mM}^{-1}$ ). It also converts unusual bulky substrates with several aromatic rings (Daniel et al., 2014). The different catalytic properties of DmmA as compared to DadB, which also possesses a large active site cavity, could be the absence of tunnel bottleneck, making the active site of DmmA readily accessible to a wide spectrum of diverse substrates (Buryska et al., 2018). Protein engineering studies of HLDs have demonstrated that opening of the active site promotes the accessibility of substrate molecules, but in the cost of lowered catalytic efficiency (Brezovsky et al., 2016; Pavlova et al., 2009).

Several of the newly discovered HLDs from marine environment show useful kinetic properties, such as high affinities toward substrates or turnover numbers. Rational mutagenesis followed by kinetic analysis might reveal the molecular basis behind their activities. Natural HLDs usually exhibit only a moderate catalytic efficiency in  $10^4\text{--}10^5\text{M}^{-1}\text{s}^{-1}$  range with their best substrates and significantly lower for environmental pollutants such as 1,2,3-trichloropropane, e.g.,  $40\text{M}^{-1}\text{s}^{-1}$  for DhaA (Koudelakova, Bidmanova, et al., 2013). Improvement of the HLD catalytic efficiency by protein engineering has proven to be a valuable tool for obtaining efficient catalysts for biotechnological applications (Dvorak, Bidmanova, et al., 2014; Dvorak, Kurumbang, et al., 2014; Pavlova et al., 2009).

### 3.3 Enantioselectivity

The production of enantiopure compounds has become an expanding area of research, especially for pharmaceutical, agrochemical, and food additive industries, where high enantiomeric purities are required (Kokkonen et al., 2017). Several well-characterized HLDs, namely DhaA, LinB, DbjA, DatA, DpcA, and DbeA, have shown high magnitude of chiral recognition ( $E$ -value  $> 200$ ) for  $\alpha$ -brominated esters (Chaloupkova et al., 2014; Drienovska, Chovancova, Koudelakova, Damborsky, & Chaloupkova, 2012; Hasan et al., 2011; Prokop et al., 2010). The same high level of enantioselectivity toward  $\alpha$ -bromoamides was found for DbjA, LinB, DhaA, and its engineered variant DhaA31 (Westerbeek et al., 2011). DbeA, DatA, and DbjA also exhibit high enantioselectivity toward selected  $\beta$ -brominated alkanes (Chaloupkova et al., 2014; Hasan et al., 2011; Prokop et al., 2010).

Excellent enantioselectivity ( $E$ -value  $> 200$ ) toward a racemic mixture of ethyl 2-bromopropionate was measured for marine dehalogenases DmxA (Chrast et al., 2018), DpaA, and DpaB (Vanacek et al., 2018), while considerably high enantioselectivity ( $E$ -value = 106) was observed for DmmA (Buryska et al., 2018). DpaA and DmxA exhibit enantioselectivity toward 2-bromopentane with  $E$ -values 85 and 100, respectively (Chrast et al., 2018; Vanacek et al., 2018). The only other marine HLD that shows enantioselectivity toward racemic mixtures of  $\beta$ -bromoalkanes, namely 2-bromobutane and 2-bromopentane with  $E$ -values 52 and 29, is DspA from *S. purpuratus* (Fortova et al., 2013). All enantioselective HLDs tested so far exhibit the preference for (*R*)-brominated substrates (Koudelakova, Bidmanova, et al., 2013).

Precise modulation of an enzyme structure for enhanced enantioselectivity represents one of the most important and difficult tasks of protein engineering. A recent study showing two distinct mechanisms of enantioselectivity of two HLDs corroborates the complexity of molecular recognition (Liskova et al., 2017).

### 3.4 Structure and Stability

#### 3.4.1 Analysis of Crystal Structures

Structures of four HLDs from the marine environment, namely DmmA (PDB ID: 3U1T (Gehret et al., 2012)), DppA (PDB ID: 2XT0 (Hesseler et al., 2011)), HanR (PDB IDs: 4BRZ, 4C6H (Novak et al., 2014)), and DmxA (unpublished results), have been determined by X-ray crystallography. Structures are composed of an  $\alpha/\beta$ -hydrolase main domain and the

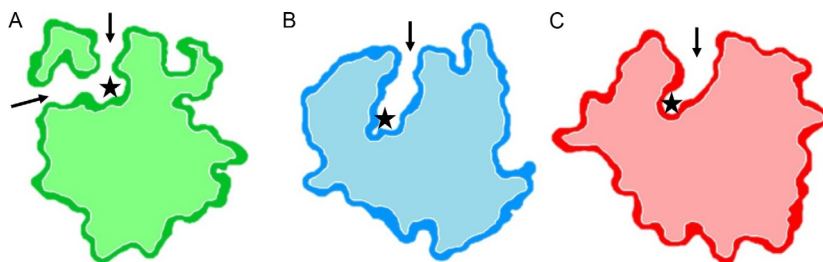


**Fig. 1** Schematic view of marine HLDs access tunnels. (A) DmmA (green), (B) HanR (blue), and (C) DppA (red). Tunnels connecting the buried active site with the enzyme surface are depicted by black arrows. Active site of each enzyme is marked with a black star. Note that two wide tunnels and open active site of DmmA form a groove on the cross-section.

helical cap domain, with active site cavity located at their interface (Janssen, 2004). The size of the active site cavity and entry tunnels connecting it with the enzyme surface play role in the substrate specificity (Koudelakova et al., 2011) and enantioselectivity (Prokop et al., 2010).

The analysis of DmmA structure revealed a wide tunnel opening and the large active site cavity compared to other HLD homologues (Fig. 1) (Gehret et al., 2012). These structural features determine its broad substrate specificity and capability of utilizing large and bulky substrates (Buryška et al., 2018). The differences in substrate preference between highly similar enzymes from HLD-II group were resolved by the comparison of their substrate binding pockets. Substitution of I138 and M253 (LinB) to corresponding residues R136 and V252 in HanR creates space to which substrates with longer chains can be accommodated (Novak et al., 2014).

The inability of DppA to convert chlorinated substrates can be explained using the comparison of its structure and sequence with DhIA, which has 50% sequence identity and is phylogenetically close to DppA. DhIA has two short-sequence repeats at the N-terminal beginning of the cap domain, which presumably evolved from a common HLD ancestor, and is responsible for activity toward 1,2-dichloroethane (Janssen et al., 2005; Pikkemaat & Janssen, 2002). The fact that DppA lacks these repeats agrees with the observation that DppA does not convert chlorinated substrates. Moreover, docking of 1-chlorobutane to the active site showed that the distance between chloride and nucleophiles of the catalytic residues is high, which could be the reason why this substrate is not converted and acts as a competitive inhibitor of the DppA (Hesseler et al., 2011).

### 3.4.2 Quaternary Structure

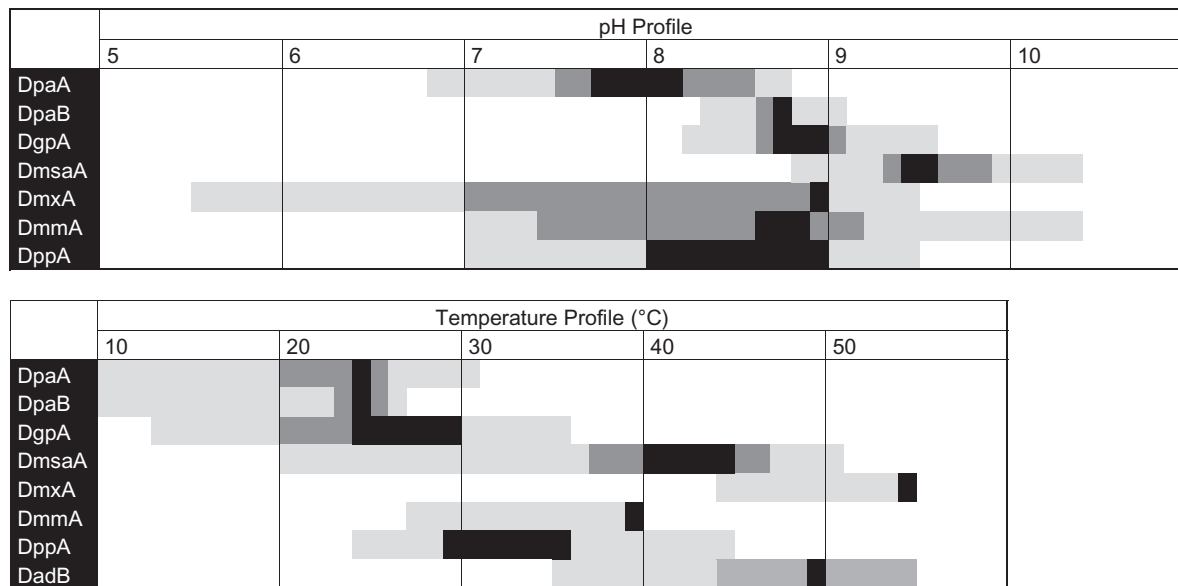
In general, HLDs can adopt various oligomeric states but mostly display monomeric form. The exceptions are enzymes from HLD-III group that form high-order multimeric structures (Jesenska et al., 2009), and DbjA, for which the oligomeric state is pH dependent. DbjA can exist as a monomer, a dimer, or a tetramer (Chaloupkova et al., 2011). A similar observation has been made for marine dehalogenases. DspA exists as a dimer in the absence of salt, but is predominantly monomeric in the presence of 0.15 M NaCl (Fortova et al., 2013). DmmA was shown to exist in a dynamic equilibrium between monomer and dimer, with most of the protein molecules (~95%) forming dimers (Burycka et al., 2018; Gehret et al., 2012). Finally, DmxA forms a dimer that is facilitated by a disulfide bridge between surface-exposed C294 residues (Chrast et al., 2018).

### 3.4.3 Effects of pH, Temperature, and Solvents on Conformational Stability

Marine HLDs display pH maxima between 7.8 and 9.5 with most retaining activity in the broad range of pH (5–10), similar to other HLDs. Temperature profiles of marine HLDs correlate with the preservation of their structure at a given temperature (Table 3). Generally, the gradual increase of activity is observed with increasing temperature followed by a sudden drop shortly after temperature optimum, corresponding to the depletion of native conformation.

The apparent melting temperature of marine HLDs is between 37°C and 66°C and most of them are within the range of other HLDs (Kokkonen et al., 2017). DmxA displays the highest apparent melting temperature of all HLDs, which is surprising due to the psychrophilic nature of its native organism. The extraordinary stability of the enzyme was owed to the very narrow and closed active site access tunnels. Mutation Q40N and opening the tunnel by mutating tunnel-gating residues M177 and F246 to smaller alanine resulted in 11°C drop of apparent melting temperature, effectively explaining the unusual stability of DmxA (Chrast et al., 2018).

The tolerance of HLDs to organic solvents is of great interest since the hydrophobic substrates dissolve easily and their presence can even increase the enzyme's enantioselectivity (Stepankova, Damborsky, & Chaloupkova, 2013). The HLD efficiency is altered in the presence of organic solvents due to changes of HLD conformation and flexibility, solvation of active site, energetics of substrate desolvation, different orientation of substrate in the

**Table 3** Temperature and pH Profiles of Selected Marine HLDs

Conditions for each measurement differ between individual HLDs and can be found in the respective publications.

Data adapted from Vanacek, P., Sebestova, E., Babkova, P., Bidmanova, S., Daniel, L., Dvorak, P., et al. (2018). Exploration of enzyme diversity by integrating bioinformatics with expression analysis and biochemical characterization. *ACS Catalysis*, 8(3), 2402–2412; Chrast, L., Tratsiak, K., Daniel, L., Sebestova, E., Prudnikova, T., Brezovsky, J., et al. (2018). Structural basis of paradoxically thermostable dehalogenase from psychrophilic bacterium. 1–38 (under review); Buryska, T., Babkova, P., Vavra, O., Damborsky, J., & Prokop, Z. (2018). A haloalkane dehalogenase from a marine microbial consortium possessing exceptionally broad substrate specificity. *Applied and Environmental Microbiology*, 1–32; Hesseler, M., Bogdanovic, X., Hidalgo, A., Berenguer, J., Palm, G. J., Hinrichs, W., et al. (2011). Cloning, functional expression, biochemical characterization, and structural analysis of a haloalkane dehalogenase from *Plesiocystis pacifica* SIR-1. *Applied Microbiology and Biotechnology*, 91(4), 1049–1060. <https://doi.org/10.1007/s00253-011-3328-x> and Li, A., Shao, Z. (2014). Biochemical characterization of a haloalkane dehalogenase DadB from *Alcanivorax dieselolei* B-5, *PLOS ONE*, 9(2), e89144. <https://doi.org/10.1371/journal.pone.0089144>.



active site, and competitive inhibition by the organic solvent molecules (Stepankova, Khabiri, et al., 2013).

Tolerance of marine DmmA toward acetone, dimethyl sulfoxide (DMSO), and methanol was assayed by monitoring changes in apparent melting temperature and activity with increasing concentration of these solvents. The enzyme is structurally tolerant to 50%, 10%, and 20% (v/v) concentrations of DMSO, acetone, and methanol, respectively. The results from the steady-state kinetics of DmmA with 4-bromobutyronitrile in the presence of these cosolvents suggest that the cosolvent binds into the active site and competes with the substrate (Burycka et al., 2018).

Several HLDs identified in the marine environment can tolerate broad pH conditions, the presence of organic cosolvents, and have exceptionally high thermal stability. The identification of biocatalysts with such interesting structural properties comes as no surprise, considering the diversity of the marine environment. Their further exploration together with protein engineering will hopefully lead to more stable biocatalysts that will be widely applicable.



## 4. EXPERIMENTAL CHARACTERIZATION OF HLDs

HLDs have been studied for more than 30 years and belong to one of the best-characterized enzyme families. Their biophysical properties, structure–function relationships, and biotechnological applications have been covered by recent comprehensive reviews (Janssen, 2004; Kokkonen et al., 2017; Koudelakova, Bidmanova, et al., 2013; Koudelakova, Chaloupkova, et al., 2013; Nagata, Ohtsubo, & Tsuda, 2015). The following section gives an overview of methods that are used for analysis of biochemical and biophysical properties of HLDs.

### 4.1 Expression and Purification

HLDs are routinely expressed in a soluble and active form in *E. coli* BL21(DE3) strain from pET-based vectors (pET21a,b, pET22b, pET24a, pETM11) inducible by isopropyl- $\beta$ -D-1-thiogalactopyranoside. Codon optimization for *E. coli* generally results in higher yields. Target proteins are purified using metal affinity chromatography using immobilized  $\text{Ni}^{2+}$  or  $\text{Co}^{2+}$ , and six histidines commonly attached to the C-terminus. DmmA is expressed using pET24a where the His-tag is positioned on N-terminus (Burycka et al., 2018). The presence of His-tag does not show a significant effect on activity

or stability, and therefore, there is no need to cleave it from the purified protein. In most cases, one-step metalloaffinity purification is sufficient for high purity (>90%–95%) and good yields (60–280 mg of protein from 1 L of bacterial culture grown in LB media). These amounts are sufficient for standard biochemical and biophysical assays. Additional purification step using ion-exchange or size-exclusion chromatography may be carried out when purity after the first purification is low and is recommended when the downstream application requires highly pure and homogenous sample, e.g., for protein crystallization.

The obvious exception is HLD-III subgroup (Chovancova et al., 2007). These proteins, namely DrbA, DmbC (Jesenska et al., 2009), DmrB (Fung et al., 2015), DhmeA (Vanacek et al., 2018), and DhcA (unpublished results) display low solubility, poor yields, and low purity. Currently, several strategies are being employed to increase yield and obtain homogeneous proteins: (i) variation of expression strains, (ii) different cultivation media, (iii) purification conditions, and (iv) different purification tags. The optimization of HLD-III expression and purification protocols is challenging, but is essential for the determination of their tertiary structures by X-ray crystallography and quaternary structure by cryoelectron microscopy.

## 4.2 Specific Activity

HLDs possess broad substrate specificity, with more than 100 halogenated compounds reported as substrates (Nagata et al., 2015), including monochlorinated, brominated, and iodinated n-alkanes, multihalogenated n-alkanes, haloalkenes, haloalcohols, halohydrins, cyclohaloalkanes, haloethers, haloesters, haloacetamides, and haloacetonitriles (Damborsky et al., 2001). A classification system that divides HLDs into 4 substrate specificity groups based on their activity with 30 representative substrates has been proposed by Koudelakova et al. (2011). Some of these compounds are highly toxic, corrosive, volatile, and poorly soluble in water (Table 2). Five halogenated compounds, 1-bromobutane, 1-iodopropane, 1-iodobutane, 1,2-dibromoethane, and 4-bromobutyronitrile, were identified as universal substrates applicable for the screening of HLD activity. 1,2-Dichloroethane, 1,2-dichloropropane, 1,2,3-trichloropropane, chlorocyclohexane, and (bromomethyl)cyclohexane, on the other hand, are considered poor substrates, and biocatalysts capable of their degradation are of special interest (Koudelakova et al., 2011).

The hydrolysis of halogenated compounds by HLDs yields a corresponding alcohol, a halide ion, and a proton, and all three products are used for the activity detection. A spectrophotometric detection of halides described by Iwasaki, Utsumi, and Ozawa (1952) and later modified by Zall, Fisher, and Garner (1956) and Bergmann and Sanik (1957) is widely used for monitoring halide release during dehalogenase reactions (Keuning et al., 1985). Other methods for halide detection include capillary electrophoresis (Glatz, Marini, Wimmerova, Damborsky, & Nagata, 2000), ion-specific electrodes (Janssen et al., 1988), and fluorescence quenching (Marchesi, 2003). Change in pH during the enzymatic reaction can be monitored by absorbance-based (Holloway, Trevors, & Lee, 1998; Zhao, 2003) or fluorescence-based (Bidmanova et al., 2010) indicators. The precise measurement of substrate or alcohol product, which enables kinetic and enantioselectivity measurements, is carried out using gas chromatography (GC) coupled with a mass spectrometer (Curragh et al., 1994), an electron capture detector (Arbon & Grimsrud, 1990), or a flame ionization detector (Schanstra, Kingma, & Janssen, 1996). Additionally, conversion of an alcohol product to aldehyde and hydrogen peroxide by alcohol oxidase and subsequent detection of hydrogen peroxide via horseradish peroxidase-catalyzed oxidation of a chromogenic substrate have also been used for the detection of dehalogenase activity (Fabritz et al., 2012). Finally, several fluorogenic substrates of HLDs have been discovered and synthesized for detection of dehalogenase activity in high-throughput screening assays, but further optimization and testing must be done before their broader utilization is possible (unpublished data). In this section, three main methods for determination of HLD activity are described: (i) colorimetric assay, (ii) gas chromatography assay, and (iii) pH assay.

#### **4.2.1 Colorimetric Assay**

The colorimetric assay based on spectrophotometric detection of halides is routinely used for measurement of HLD activity and substrate specificity (Damborsky et al., 2001; Drienovska et al., 2012; Hasan et al., 2011; Hesseler et al., 2011; Jesenska et al., 2002, 2009, 2005; Keuning et al., 1985; Pavlova et al., 2009; Sato et al., 2005; Schanstra et al., 1996), temperature and pH profiles (Jesenska et al., 2002, 2009, 2005), functional half-lives at elevated temperatures (Gray et al., 2001), and effects of organic solvents on HLD activity (Stepankova, Damborsky, et al., 2013; Stepankova, Khabiri, et al., 2013; Stepankova, Vanacek, Damborsky, & Chaloupkova, 2014).

The disadvantage of this method is the use of highly toxic reactants and corrosive chemicals (e.g., nitric acid). Moreover, the assay is not suitable for “online” monitoring of the reaction since it requires sampling and sample preparation for the coupled chemical reaction producing the signal.

#### 4.2.1.1 Principle

The assay is based on the displacement of thiocyanate from its salt by halide ions and its subsequent detection by the formation of a colored complex with iron(III) ions (Iwasaki et al., 1952) according to the following reaction scheme:



( $X^- = \text{Cl}^-$ ,  $\text{Br}^-$ , and  $\text{I}^-$ )

#### 4.2.1.2 Chemicals

- Detection solution I: 28.4 mM  $\text{Hg}(\text{SCN})_2$  in ethanol (>99%, HPLC grade), filter 0.22  $\mu\text{m}$  pore size
- Detection solution II: 0.56 M  $\text{NH}_4\text{Fe}(\text{SO}_4)_2 \cdot 12\text{H}_2\text{O}$  in 21%  $\text{HNO}_3$ , filter (0.22  $\mu\text{m}$  pore size)
- Calibration solutions: 1 M solutions of NaCl, NaBr, and KI in deionized  $\text{H}_2\text{O}$
- Reaction buffer (100 mM glycine, pH 8.6)
- Enzyme solution
- Halogenated substrate
- Nitric acid (35%)

#### 4.2.1.3 Material and Equipment

- Glass syringes (0.01, 0.5, and 1 mL volumes)
- Shaking water bath with temperature control
- Gas-tight reaction flask with syringe access
- Microcentrifuge tubes
- 96-Well microplate
- Absorbance plate reader

#### 4.2.1.4 Calibration

1. Prepare dilution series of each halide solution in 0–1 mM range.

2. Pipet 1 mL of each solution to the microcentrifuge tubes containing 0.1 mL of 35%  $\text{HNO}_3$ , 0.1 mL of detection solution I, and 0.2 mL of detection solution II, and mix thoroughly.
3. Pipet 0.1 mL of each solution into the microtiter plate (six replicates) and measure absorbance at 460 nm ( $A_X$ ).
4. Repeat steps 2 and 3 with 1 mL of deionized water instead of the halide solution ( $A_{\text{Blank}}$ ).
5. Construct the calibration curve by plotting the average absorbance values corrected for background absorbance ( $A_X - A_{\text{Blank}}$ ) vs concentration of halides (Fig. 2A).
6. Repeat the procedure for each halide.

#### 4.2.1.5 Procedure

1. Inject 10  $\mu\text{L}$  of tested substrate into 10 mL of reaction buffer in reaction flask closed by gas-tight caps with syringe access.
2. Mix thoroughly and incubate in water shaking bath at reaction temperature for 30 min.
3. Prepare “enzyme blank” using 2.25 mL of reaction buffer and 0.05 mL of enzyme solution ( $((V_{\text{reaction buffer}} - 1 \text{ mL})/4 + V_{\text{enz.}}/4)$ ). Mix 1 mL of this buffer–enzyme solution with 0.1 mL of 35%  $\text{HNO}_3$  in a microcentrifuge tube ( $B_{\text{enzyme}}$ ).
4. Prepare “buffer blank” by mixing 1 mL of the reaction buffer with 0.1 mL of 35%  $\text{HNO}_3$  in a microcentrifuge tube ( $B_{\text{buffer}}$ ).

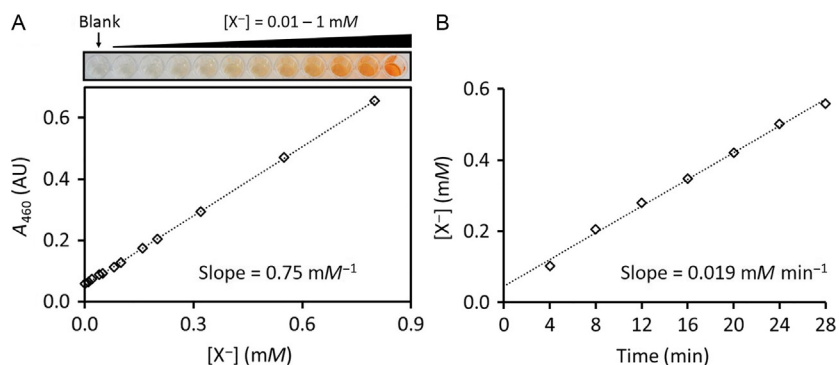


**Fig. 2** Colorimetric assay for measurement of HLD activity. (A) Example of calibration using NaBr. (B) Plot of halide concentration vs time. Slope of the plot divided by the enzyme concentration provides a specific activity. Concentration of halides formed during HLD reaction is calculated from the absorbance using the slope from a calibration curve.

5. Draw 1 mL from the reaction mixture before adding the enzyme and mix it with 0.1 mL of 35%  $\text{HNO}_3$  in a microcentrifuge tube ( $B_0$ ).
6. Start reaction by adding 0.2 mL of enzyme solution.
7. Withdraw 1 mL of the reaction mixture periodically to microcentrifuge tubes with 0.1 mL of 35%  $\text{HNO}_3$  and mix thoroughly to terminate the reaction. Sample the reaction at least six times.
8. Add 0.1 mL of detection solution I and 0.2 mL of detection solution II to each microcentrifuge tube (including blanks) and mix thoroughly.
9. Pipet 0.1 mL from each tube to the microtiter plate (eight replicates).
10. Measure the absorbance of each well at 460 nm and calculate the average values.
11. Correct the absorbance value of each point during reaction for background absorbance ( $A_{\text{back.}} = A_{\text{enzyme}} + A_0 - A_{\text{buffer}}$ ).
12. Recalculate the absorbance values from step 11 to product concentration using slope of the calibration curve of the analyzed halide (Fig. 2B).
13. Convert the specific activity to  $\mu\text{mol s}^{-1} \text{mg}^{-1}$  of protein.

#### 4.2.1.6 Notes and Troubleshooting

- Avoid using reaction buffers containing halides or components that may interfere with the assay (e.g., buffered saline solutions, Tris-HCl, etc.). Check the possible interference of buffer components by preparing the calibration curve in the reaction buffer. Glycine buffer (100 mM, pH 8.6) is commonly used for the measurement of specific HLD activity.
- Volumes can be adjusted according to the need. Nonetheless, the substrate:buffer ratio should always be 1:1000.
- Enzyme concentration and reaction time must be adjusted so that the response of released halides is in the range of the calibration curve.
- Correction for abiotic dehalogenation must be done in cases where spontaneous hydrolysis of the substrate occurs.

#### 4.2.2 Gas Chromatography Assay

Monitoring of substrate and/or product concentration during enzymatic reaction is arguably the most accurate method how to analyze catalytic performance of HLDs enabling evaluation of specific activity, kinetic, and/or stereoselectivity (Bohac et al., 2002; Jesenska et al., 2005; Nagata et al., 2003, 2005; Oakley et al., 2002; Pieters, Lutje Spelberg, Kellogg, & Janssen, 2001). The halogenated substrate and corresponding alcohol product are extracted from the aliquots of the reaction mixture to organic solvent (e.g., diethyl ether, hexane, acetone) containing an internal standard (ISTD, halogenated

compound with similar analytical response to the analyte) to correct for the loss of analyte during sample preparation or deviation caused by injection procedure. Injected sample is vaporized and separated on gas chromatography columns. Individual components are analyzed using flame-ionization, electron-capture, or mass spectrometer detectors and subsequently quantified from calibration curve with internal standard. Alternatively, the analysis can be carried out by direct injection of the aqueous reaction mixture (using column resistant to aqueous samples) or by analysis of a mixture of the aqueous sample with organic cosolvent (e.g., methanol). The concentration of substrates/products must be corrected for the abiotic hydrolysis of the substrate measured in the reaction with the thermally inactivated enzyme or in its complete absence.

#### 4.2.2.1 Material and Equipment

- Organic solvent immiscible with water (hexane, diethyl ether, acetone); HPLC grade
- Halogenated substrate
- An internal standard (a stable halogenated compound with similar instrumental response to the analyte)
- Enzyme solution (concentration must be optimized with respect to HLD activity)
- Reaction buffer (mild alkaline buffers, e.g., glycine, Tris-HCl)
- Shaking water bath with temperature control
- Gas-tight reaction flask with syringe access
- GC vial (2 mL volume) with a crimp cap
- Gas chromatograph equipped with flame-ionization, electron-capture, or mass spectrometer detectors
- Glass syringes

#### 4.2.2.2 Calibration

1. Prepare extraction solution by dissolving 100  $\mu$ L of internal standard (ISTD; halogenated compound) in 100 mL of organic solvent (e.g., diethyl ether, hexane, acetone).
2. Dissolve 1  $\mu$ L of commercially available substrate (product) in 1 mL of the extraction solution.
3. Calculate the concentration of the substrate (product) in the extraction solution using its molecular weight and density.
4. Make a serial dilution of substrate (product) solution from step 2 to the extraction solution in 1:1 ratio (at least five concentrations).

5. Inject 1  $\mu\text{L}$  of each calibration sample to the GC column with polar phase.
6. Create a calibration curve by plotting the ratio of substrate (product) to ISTD response vs substrate concentration.
7. Repeat procedure with all tested substrates (products).

#### 4.2.2.3 Procedure

The reaction is carried out in the same experimental setup as described in the protocol for colorimetric assay with following exceptions:

- Periodically withdraw 0.5-mL aliquots from the reaction mixture during the reaction and mix with 0.5 mL of extraction solution (used for the preparation of calibration curves) to terminate the reaction. Collect the samples to GC vials (with an insert if needed) enclosed by a crimp cap.
- Inject 1  $\mu\text{L}$  of extraction solution to sample injector and separate substrates, products, and ISTD on GC column.
- Calculate the concentration of substrate (product) at each time point from the calibration curve.
- Subtract the abiotic control from the rate of the substrate/product concentration.
- Quantify dehalogenation activity either as a rate of substrate decrease or alcohol product formation in time (Fig. 3).

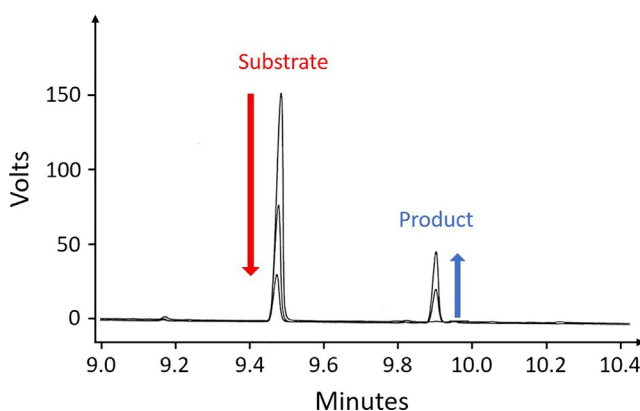


**Fig. 3** Example of gas chromatogram from the measurement of HLD activity with a halogenated substrate. As the reaction proceeds the amount of substrate is decreasing and the corresponding alcohol product is formed.



#### 4.2.2.4 Notes and Troubleshooting

- This approach is also used for measurement of steady-state kinetics or stereoselectivity of HLDs. For steady-state kinetics, the initial rates of dehalogenation are measured at different substrate concentrations to generate the Michaelis–Menten curve. For stereoselectivity analysis, the conversion of a mixture of isomers is analyzed by using GC equipped with a chiral column providing a separate detection for all involved stereoisomers.
- The internal standard should have a similar signal as the analyte, while distinguishable by the analytical method (1,2-dichloroethane is commonly used).
- All liquid handling steps can be automated by robotic autosamplers, which allows performing sample preparation and analysis in a high-throughput format.

#### 4.2.3 pH Assay

The pH indicator assays (Holloway et al., 1998; Zhao, 2003) are quick and easy and can be adapted for screening of HLD activity in whole cells or cell-free extracts (Dörr et al., 2016; Jesenska, Sedlacek, & Damborsky, 2000; Sharma et al., 2014), in directed evolution studies (Gray et al., 2001; Pavlova et al., 2009; Tang, Li, & Wang, 2010), or in extensive characterization studies (Marvanova et al., 2001; Schindler et al., 1999).

The reaction is carried out in weak buffer (e.g., 1 mM HEPES, 20 mM sodium sulfate, pH 8.2) containing phenol red ( $20\text{ }\mu\text{g mL}^{-1}$ ). The substrate is added in sufficient amount to ensure that the reaction proceeds in maximum velocity and the reaction mixture is incubated for 30 min in the gas-tight flask. The assay mixture is distributed in equal amounts into the microtiter plate wells, and the reaction is started by addition of enzyme (concentration must be optimized for each enzyme–substrate reaction so that the resulting change in absorbance is in the range of the calibration curve). The enzyme must be dialyzed against reaction buffer prior the measurement. The decrease of absorbance at 560 nm is measured over time and the resulting kinetic data are used for the quantification of the dehalogenase activity. The enzymatic dehalogenation must be corrected for the abiotic substrate hydrolysis that is measured in the same way with the temperature-inactivated enzyme (Marvanova et al., 2001).

Different compounds sensitive to pH change have been used to monitor dehalogenation by purified enzymes or in cells and cell-free extracts. Fluorescence or absorbance indicators can be rapidly used in online assays

involving microfluidics, on agar plates to distinguish between degrading and nondegrading colonies (Loos, 1975; Zhao, 2003) or for detection of toxic compounds in situ (Bidmanova et al., 2010, 2016). The disadvantage of pH assays for determination of substrate specificity is buffer limitation and use of “open” systems (microtiter plate) that can, however, be overcome by using a lid with a hydrophobic coating to prevent evaporation of the substrate.

#### 4.2.4 Overview

The selection of a technique should always be made with respect to the materials and equipment available in the laboratory, speed, and level of information one needs to obtain from the measurement. An assay based on a pH change is the most suitable for initial and fast screening of dehalogenase activity. Gas chromatography must be used when the concentration of substrates and products needs to be determined at low levels or with high accuracy and MS detection if the identity of the product needs to be determined. Iwasaki method is arguably the most universal and is routinely used for determination of activity, substrate specificity, monitoring of functional half-life, as well as temperature and pH profiles (Damborsky et al., 2001; Drienovska et al., 2012; Gray et al., 2001; Hasan et al., 2011; Hesseler et al., 2011; Jesenska et al., 2002, 2009, 2005; Keuning et al., 1985; Pavlova et al., 2009; Sato et al., 2005; Schanstra et al., 1996).

Currently, there are no suitable assays for screening large libraries of HLD variants in cells or microfluidic droplets. The use of existing pH indicators is often hindered by their physiochemical properties. Although fluorescent indicator has been recently developed for monitoring environmental pollutants in the environment (Bidmanova et al., 2016), its use in high-throughput screening assay must be further optimized. Alternatively, the discovery of fluorescent substrates that can be utilized by HLDs would be beneficial for high-throughput screening projects aiming to either discover new HLDs or improve properties of characterized HLDs by protein engineering endeavors. Several potential fluorescent substrates have been identified using *in silico* screening, giving experimental grounds for their further use in the experimental screening projects (Daniel et al., 2014).

### 4.3 Steady-State Kinetics

Although specific activities provide important information about the specificity of each enzyme, detailed kinetic characterization of enzyme reaction and mechanism is crucial for the understanding of enzyme function.

The kinetic analysis allows identification of reaction intermediates, determination of rate-limiting steps along the reaction pathway, and evaluation of enzyme specificity and function based on the quantitative analysis of binding energies and turnover numbers. The understanding of enzyme catalytic mechanism on a molecular level is key to exploiting and harvesting natural biocatalyst for biotechnological or medicinal purposes. The kinetic resolution of individual steps is possible using rapid stopped-flow or quench-flow methods and obtained information can be subsequently used to enhance desired enzymatic properties by protein engineering (Brezovsky et al., 2016; Pavlova et al., 2009). However, the description of this method is beyond the scope of this chapter and authors refer readers to Bosma, Pikkemaat, Kingma, Dijk, and Janssen (2003), Prokop et al. (2003), and Schanstra et al. (1996) for further reading on this topic.

The selection of a technique for determination of HLD steady-state kinetic parameters is largely affected by chemical properties of the substrates. Hydrophobicity, low solubility, and high volatility of these compounds are major drawbacks that do not allow direct determination of their concentration by simple calculation and dilution. Instead, a precise analytical method such as gas chromatography must be used for this purpose.

The standard steady-state kinetics are evaluated from the dependence of the initial rates estimated at varying substrate concentrations using methods described in a previous section (Bohac et al., 2002; Janssen et al., 1988; Schindler et al., 1999). The substrate concentration needs to be significantly higher than the enzyme concentration during measurement, so it can be approximated to be constant. Moreover, it is important to quantify the rates from the early stages of the reaction so that the rates of reverse reactions are negligible.

The alternative to measurement of steady-state kinetic data by discontinuous initial rate estimation is the total conversion methods which calculate an instantaneous differential rate at each time of progress conversion curve. This method needs to count with significant effects of product inhibition since all starting substrate is fully converted to the product during the analysis. The progress curves can be recorded by numerous techniques mentioned earlier (e.g., GC, spectrophotometry) or by using advanced methods like isothermal titration calorimetry (ITC).

ITC measures the rate of heat change during the enzyme-catalyzed reaction and is therefore universally applicable without the need of any spectroscopic requirements of the reactants, no chemical modifications or labeling, coupling reaction, or an analytical method for separation and quantitation of

products. An enzyme can be (i) titrated with increasing amounts of substrate, while maintaining the pseudo-first-order conditions or (ii) the change in thermal power upon single substrate injection can be continuously monitored as the substrate is depleted by the enzyme. Both methods allow highly precise kinetic characterization in a single experiment and can be used to measure enzyme inhibition (Todd & Gomez, 2001). Since ITC represents a promising universal technique for determination of steady-state kinetic parameters of HLDs, a basic introduction and experimental procedures are given in the following text.

#### 4.3.1 Isothermal Titration Calorimetry

ITC is commonly used to characterize thermodynamics of macromolecule-binding interactions and kinetics of enzyme-catalyzed reactions (Freyer & Lewis, 2008). ITC enables the measurement of kinetic parameters of a wide variety of enzymatic reactions without any modifications or labeling, providing that the reaction is associated with detectable heat change (modern ITC measures heat effects as small as  $0.1 \mu\text{cal}$  and heat rates  $0.1 \mu\text{cal s}^{-1}$  (Freyer & Lewis, 2008)). This method is routinely used to characterize reaction mechanism and catalytic efficiency of HLDs (Babkova, Sebestova, Brezovsky, Chaloupkova, & Damborsky, 2017; Liskova et al., 2015; Monincova, Prokop, Vevodova, Nagata, & Damborsky, 2007; Prokop et al., 2003; Vanacek et al., 2018). Moreover, it proved to be an invaluable tool for analysis of HLD inhibition kinetics (Buryška et al., 2016; Prokop et al., 2003).

The amount of heat change during conversion of  $n$  moles of the substrate to product is equal to the product concentration multiplied by reaction volume (cell volume) and apparent enthalpy change of the reaction ( $\Delta H_r$ ). Moreover, the thermal response of ITC instrument is directly proportional and can be recalculated to the rate of reaction. Enthalpy change of the reaction is measured in a separate experiment with high concentration of enzyme (approx. 10 times higher) and longer spacing between injections to allow complete conversion of the injected substrate. The reaction heat is calculated by dividing the area of the peak by the amount of substrate (Hansen, Transtrum, Quinn, & Demarse, 2016).

Steady-state kinetics of HLDs with substrates that produce a low amount of heat during their conversion to products or with poorly soluble substrates (e.g., 1-bromobutane, 1-iodobutane, bromocyclohexane; see Table 1) must be measured using a single injection mode. In this experimental setting, the enzyme is injected into the cell containing substrate solution and complete

conversion of the substrate is analyzed. The value of  $\Delta H_r$  is determined by integration of the thermogram according to the following equation:

$$\Delta H_r = \frac{\int_{t=0}^{\infty} \frac{dQ}{dt} dt}{[S]_0 V_{\text{cell}}}$$

where  $dQ/dt$  is the reaction heat rate,  $[S]_0$  is the initial concentration of substrate, and  $V_{\text{cell}}$  is the volume of the calorimetric cell. The estimation of kinetic parameters in the single injection more involves more complex analysis. Extensive and detailed description of the analytical procedure can be found elsewhere ([Freyer & Lewis, 2008](#); [Hansen et al., 2016](#)).

Here, a protocol for measurement of the steady-state kinetics of haloalkane dehalogenases by ITC using multi-injection mode is described. For a comprehensive description of ITC theory, practice, and experimental considerations, see the following relevant literature: [Frasca \(2016\)](#), [Freyer and Lewis \(2008\)](#), and [Todd and Gomez \(2001\)](#).

#### 4.3.1.1 Material and Equipment

- ITC instrument (cell and injector volumes in this protocol are based on VP-ITC instrument, Malvern, UK)
- Glass syringe
- Reaction buffer (use buffer with low ionization enthalpy, e.g., glycine, HEPES)
- Substrate solution (substrate dissolved in reaction buffer, ideally in the same buffer which was used for enzyme dialysis)
- Enzyme solution (enzyme dialyzed against reaction buffer)
- Organic solvent immiscible with water containing ISTD (preparation is described in the protocol for measurement of specific activity by GC)

#### 4.3.1.2 Measurement of Apparent Enthalpy Change of the Reaction

1. Dissolve 10  $\mu\text{L}$  of substrate in 4 mL of reaction buffer.
2. Fill the injector with 300  $\mu\text{L}$  of substrate solution.
3. Mix 0.5 mL of the remaining substrate solution with 0.5 mL of organic solvent with ISTD.
4. Determine the concentration of the substrate using gas chromatography as described in the protocol for measurement of specific activity by GC.
5. Fill the cell with 1.4 mL of enzyme solution (see notes for details).

6. Titrate enzyme to the cell in six consecutive 10  $\mu\text{L}$  injections. Set enough spacing between the injections so that the whole reaction proceeds to completion (depends on enzyme efficiency and concentration).
7. Divide the integrated heat from the injection by the amount of substrate in the cell to determine  $\Delta H_r$  of the reaction. For further analysis, use an average value of  $\Delta H_r$  calculated from at least three independent injections.
8. Titrate the substrate solution to buffer with same parameters as in the experiment to determine the heat of dilution.
9. Correct the data for the heat of dilution.

#### 4.3.1.3 Multiple Titration Experiment

1. Fill the injector and cell with substrate and enzyme solution, respectively (see steps 1–3 in the previous subsection).
2. Titrate the enzyme in the reaction cell by 26–30 injections of 5–10  $\mu\text{L}$  of substrate solution in an injector with 2–3 min spacing between individual injections (see troubleshooting for details).
3. Calculate the substrate concentration at each injection using the data obtained by gas chromatography and respective cell and injection volumes.
4. Calculate the rate of heat production for each step with respect to a baseline extrapolated from data collected before the first injection occurred (initial delay phase).
5. Divide the values from step 4 by the total enthalpy change of reaction (from the previous experiment) to obtain reaction rates in  $\text{mM s}^{-1}$ .
6. Fit the plot of reaction rates vs substrate concentration by a simple or modified Michaelis–Menten function (including a possible substrate, product inhibition, or cooperativity) by nonlinear regression to obtain kinetic parameters (such as  $K_M$  and  $k_{\text{cat}}$ ) for a given reaction (Fig. 4).

#### 4.3.1.4 Notes and Troubleshooting

- Results largely depend on the protein and substrate concentration and it is imperative that they are accurately determined and should be verified using an analytical procedure. The enzyme concentration required for the experiment can differ significantly for each enzyme–substrate pair and must be optimized based on activity level and substrate solubility. However, it should always be two or more orders of magnitude higher for measurements of  $\Delta H_r$  than in multiple titration experiments.

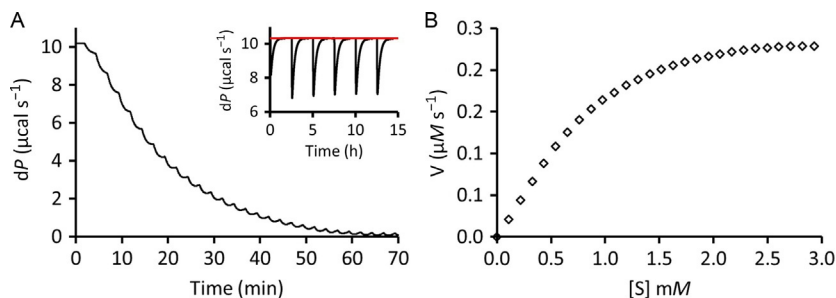


**Fig. 4** Measurement of HLD steady-state kinetics using ITC. (A) The response of the instrument during titration of the substrate to the cell containing the enzyme. *Inset:* Example of an experiment for determination of  $\Delta H_r$ , that is obtained from the average area of each peak (baseline is depicted in red) divided by the substrate concentration. (B) The plot of reaction velocity vs substrate concentration, calculated from (A) using substrate concentration and  $\Delta H_r$  as described in the text.

- Enzymes can slowly degrade in the cells during measurement which results in a continuous decrease of the peak area of each consecutive injection. In such cases, lower the reaction temperature or/and perform more experiments with fresh enzyme and fewer injections to obtain a more precise estimate of  $\Delta H_r$ .
- Buffer mismatch between enzyme and substrate can lead to artifacts caused by dilution heat induced during a mixing phase. The best solution is to exhaustively dialyze the protein and prepare the substrate solution in the resulting dialysate.
- The solubility of the substrate can be increased by the addition of DMSO (10%, v/v). Verify that it has no effect on enzyme structure and make sure that solution in cell and injector contain the same amount of DMSO.
- Raw data must be corrected for the heat of dilution of protein, substrate, and buffer by titrating each component into the buffer with same parameters as in the experiment.
- Dehalogenation reaction yields a proton that is taken up by the buffer conjugate base. Use buffers with low ionization enthalpy to suppress signal from such reaction.
- In the multiple injection mode, the spacing between injections should be set such that the signal has equilibrate before the next injection. It is important that each addition of substrate is made prior to significant reaction of the substrate so that the pseudo-first-order conditions are maintained (Freyer & Lewis, 2008).

#### 4.3.2 Overview

The steady-state kinetics is routinely accessed from initial reaction rates at different substrate concentrations measured by conventional techniques. The main disadvantage is the labor to perform many experiments required to obtain the whole kinetic dataset. ITC presents an alternative and arguably less time-consuming method of measuring HLD kinetics compared to such discontinuous assays. The specific dependence of the reaction rate on substrate concentration is easily generated from one or two automated experiments with significantly lower sample requirements. High instrument cost and the requirement for the advanced experience of the operator are the major disadvantages of the ITC technique. However, precision and sensitivity make the ITC an invaluable tool for studying not only HLD kinetics.

#### 4.4 Enantioselectivity

The application of enzymes for production of enantiopure compounds for fine chemical and pharmaceutical industry has shown to be an interesting alternative to commonly used chemical methods (Schmid et al., 2001). Two enantiomers can display different biological activity (Nguyen, He, & Pham-Huy, 2006), and therefore, the optical purity of the manufactured enantiomer should exceed the enantiomeric excess of 98% (Pollard & Woodley, 2007). In enzyme asymmetric synthesis, a prochiral precursor is selectively transformed into the desired enantiomer, whereas in kinetic resolution, enzyme preferentially converts one enantiomer from the racemic mixture faster than the other. The second enantiomer is either converted upon the depletion of the preferred one or remains unconverted. Efficient kinetic resolution of HLDs has been demonstrated for selective conversion of several  $\alpha$ -bromoesters,  $\alpha$ -bromoamides, and  $\beta$ -bromoalkanes (Prokop et al., 2010; Westerbeek et al., 2011).

Measurement of HLD enantioselectivity is carried out in 25 mL reaction flasks closed by gas-tight caps with syringe access. Racemic substrate mixture is added to the agitating buffer of choice and incubated at reaction temperature for 30 min. The enzymatic reaction is initiated by addition of the enzyme (concentration must be optimized for each substrate-HLD pair). Reaction progress is monitored by the periodical withdrawal of samples (1 mL) from the reaction mixture that are immediately mixed with diethyl ether (1 mL) containing internal standard. Samples are extracted to the organic solvent which is then subsequently analyzed using gas chromatography equipped with a chiral capillary column (Pieters et al., 2001; Prokop



et al., 2010). Equations describing competitive kinetics are fitted by numerical integration to time courses of the substrate conversion obtained from the kinetic resolution experiments to estimate the *E*-values or, alternatively, enantiomeric excess and the degree of conversion (Chen, Fujimoto, Girdaukas, & Sih, 1982).

## 4.5 Stability

The importance of protein stability for the biological function is widely recognized and can be understood as the ability of the protein to preserve its function in given conditions over time (Deller, Kong, & Rupp, 2016). High stability is of utmost importance in biotechnological applications where proteins must carry out its function for long period of time in nonnative conditions such as increased temperatures and broad pH environment, or in the presence of organic cosolvents (Bommarius & Paye, 2013). Moreover, stability is often correlated with protein evolvability (e.g., tolerance of protein to amino acid substitutions) and stable proteins are therefore important in basic research as a perfect scaffold for directed evolution studies (Bloom, Labthavikul, Otey, & Arnold, 2006). Analysis of stability is therefore essential part of protein physiochemical characterization.

Stability of HLDs is routinely assessed by a range of methods. The effect of pH, temperature, or organic cosolvents on the HLD activity can be determined: (i) in a single experiment and plotted vs the affecting factor (e.g., temperature, pH profile) or (ii) periodically monitored and expressed as a loss of activity over time at given conditions (functional half-life) (Gray et al., 2001; Jesenska et al., 2002; Stepankova et al., 2014).

The temperature unfolding of HLDs is usually partially reversible or fully irreversible and leads to an ensemble of nonfunctional conformations or aggregates. Despite this fact, protein melting temperature ( $T_m$ ), originally derived from two-state reversible denaturation model, is commonly used as a measure of HLD stability. In this context, it should be more correctly denoted as apparent  $T_m^{\text{app}}$  and understood in terms of a midpoint of observed melting transition, rather than the temperature where concentrations of native and denatured states are identical. It is suitable for comparison of stabilities among different HLDs or different variants of the same enzyme.  $T_m^{\text{app}}$  of HLDs is most commonly measured by circular dichroism (CD) or differential scanning calorimetry (DSC). Alternatively, intrinsic (Fig. 5C) or extrinsic fluorescence using SYPRO orange dye can be used for fast screening of HLD stability at low concentrations ( $\sim 0.1 \text{ mg mL}^{-1}$ ) and volumes ( $\sim 10 \mu\text{L}$ ) (Vanacek et al., 2018).

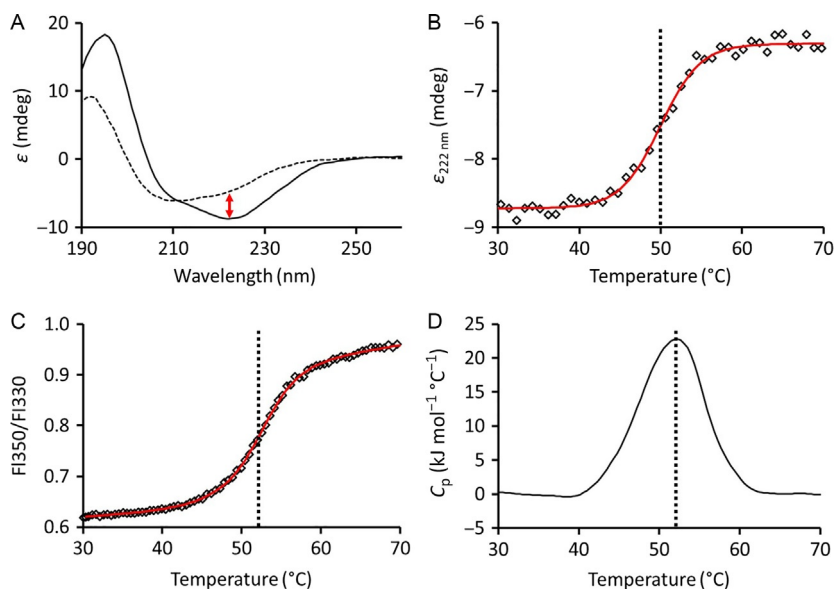


**Fig. 5** Measurement of HLD stability. (A) Typical CD spectra of native (*black line*) and unfolded (*dotted line*) HLD. (B) Depletion of HLD secondary structure during temperature scan followed by changes in ellipticity at 222 nm. Data can be fitted by sigmoidal curve (*red line*). The inflection point is usually reported as apparent melting temperature (*dotted line*). (C) Changes in fluorescence spectra of HLDs during temperature. Red-shift of fluorescence spectra can be observed from the plot of the ratio of fluorescence intensities at 350 and 330 nm vs temperature. Note that the midpoint of transition (*dotted line*) from the fit (*red line*) is 2  $^{\circ}\text{C}$  higher than in CD measurement. (D) DSC thermogram of HLDs. The figure shows baseline-subtracted data of heat capacity vs temperature. Here, maximum of the peak corresponds to the apparent melting temperature (*dotted line*). Unpublished data.

#### 4.5.1 Circular Dichroism

The  $\alpha/\beta$  hydrolase fold of HLDs produces characteristic CD spectrum in the far-UV region (180–260 nm) where the circularly polarized light is absorbed by peptide bonds forming the asymmetric secondary structure elements ( $\alpha$ -helices,  $\beta$ -sheets) (Kelly & Price, 2000). The CD spectrum of HLDs shows one maximum around 190 nm and two local minima around 208 and 222 nm (Fig. 5A), typical for  $\alpha$ -helical proteins (Fasman, 1996). During heat denaturation, the noncovalent interactions break, and secondary structure elements are gradually depleted. Protein stability can, therefore, be easily assessed by monitoring CD ellipticity at wavelengths around 222 nm as a function of temperature to obtain  $T_m^{\text{app}}$  (Fig. 5A and B), or at a fixed temperature as a function of time to determine structural half-life ( $t_{1/2}$ ).

CD spectroscopy found utility in studies examining effects of temperature, pH, cosolvents, ionic strength, or amino acid substitutions to the conformational stability of HLDs (Chaloupkova et al., 2011, 2014; Drienovska et al., 2012; Fortova et al., 2013; Hasan et al., 2011, 2013; Jesenska et al., 2009, 2005; Koudelakova, Bidmanova, et al., 2013; Koudelakova, Chaloupkova, et al., 2013; Liskova et al., 2015; Nakamura et al., 2006; Stepankova, Damborsky, et al., 2013; Stepankova et al., 2014; Sykora et al., 2014).

#### 4.5.2 Differential Scanning Calorimetry

During DSC measurement, the protein sample is gradually heated at a specified scan rate and response of the instrument is converted to protein heat capacity. During protein unfolding, heat is absorbed which results in the formation of the characteristic melting peak (Fig. 5D). The immediate parameters that can be obtained from the data without any fitting include: (i) the area under the peak, which corresponds to the amount of the heat absorbed by protein during unfolding, (ii) maximum of the peak,  $T_m^{app}$ , and (iii) onset temperature of unfolding,  $T_{onset}$ . DSC is the only technique that can directly measure heat change during protein denaturation and therefore provides valuable information about the thermodynamics and kinetics of unfolding process. The description of DSC data analysis is beyond the scope of this review and can be found elsewhere (Ibarra-Molero, Naganathan, Sanchez-Ruiz, & Muñoz, 2015; Privalov & Dragan, 2007; Privalov & Privalov, 2000). Although DSC requires a significant amount of protein for the analysis ( $\sim 1 \text{ mg mL}^{-1}$ ), it provides the most accurate description of denaturing process. It has been used to study stability of HLDs in the presence of cosolvents (Stepankova, Damborsky, et al., 2013), binding of the inhibitor to the mycobacterial HLD DmbA (Buryška et al., 2016), or the evaluation of mutations designed to enhance stability of HLD DhaA (Bednar et al., 2015). Moreover, recent comprehensive analysis of reheating scans, terminated at different temperature points, showed a surprising difference in unfolding mechanisms of three structurally similar proteins LinB, DhaA, and DbjA (Mazurenko et al., 2017). Developed methodology was incorporated to the web-based software called CalFitter (Mazurenko et al., 2018), which serves as unified platform for analysis of protein thermal denaturation data measured by temperature scanning techniques (e.g., DSC, CD, fluorescence spectroscopy) and kinetic measurements (temperature jumps) (Fig. 6).

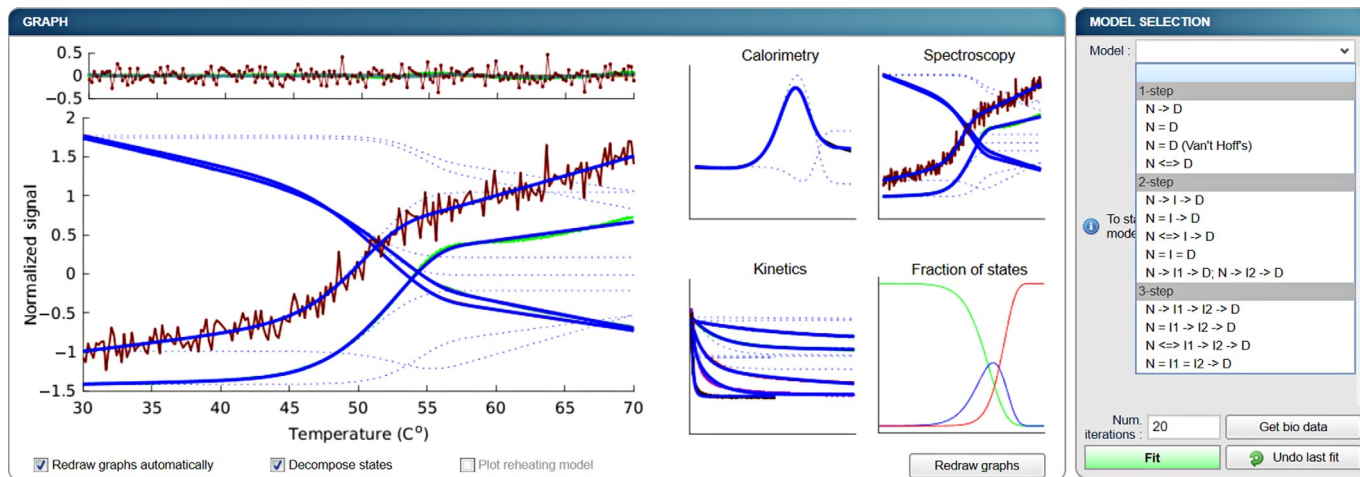


**Fig. 6** Example analysis of protein thermal denaturation data using CalFitter web. The web tool offers a variety of options for data visualization, pretreatment, simulation, and fitting. Data are visualized in the graph window (left side) and each data set can be enlarged by a mouse click. CalFitter web offers 12 different models of unfolding (right side of the figure) that can be used for fitting of data measured by spectroscopy, calorimetry, or kinetics. Software is freely available at <https://loschmidt.chemi.muni.cz/calfitter>.



## 5. CONCLUSIONS AND PERSPECTIVES

Growing demand for enzymes with novel or interesting properties have been a driving force for their discovery from diverse environments and habitats. Oceans cover more than 70% of planet surface and organisms living in the marine environment contain biochemical secrets to be discovered. HLDs are no exception. Twelve novel enzymes have been found in marine organisms in the past 8 years, adding to a total of 34 biochemically characterized members of HLD family to date (Kokkonen et al., 2017; Kotik et al., 2017; Vanacek et al., 2018). Despite the considerable amount of structural, biophysical, and biochemical information available from the analysis of wild-type HLDs and their engineered variants, there is still a lot to learn about this interesting enzyme family.

Although the diversity of organisms which express HLDs and utilize their function is large and spanning all three domains of life, the biological function of most characterized enzymes remains elusive. Presence of the same coding gene in phylogenetically different microorganisms strongly suggests an important role of horizontal gene transfer in the distribution of HLD genes among bacteria worldwide (Poelarends, Kulakov, et al., 2000; Poelarends, Zandstra, et al., 2000). This observation is further supported by the presence of genes coding for invertases or transposases and insertion sequences localized downstream and upstream of dehalogenase genes (Kulakov, Poelarends, Janssen, & Larkin, 1999; Kulakova et al., 1997; Mattes et al., 2008) that are often found as part of a catabolic gene cluster for degradation of a xenobiotic compound (Liang, Jiang, Zhang, Zhao, & Li, 2012; Nagata et al., 1999; Poelarends, Kulakov, et al., 2000; Poelarends, Zandstra, et al., 2000). The acquisition of mobile genetic elements coding for degradation pathway of a halogenated compound by bacteria provides them with a competitive advantage in a polluted environment, leading to their positive enrichment. However, the evolutionary origins of dehalogenase genes are still unknown. Sequence similarity among individual HLDs is generally low (50%), which suggests that the divergence of dehalogenase function occurred much earlier than the introduction of man-made environmental pollutants. Presumably, common dehalogenase ancestors may have evolved from other genes via mutation through long-term vertical evolution (Liang et al., 2012).

The ancestral HLD genes could catalyze a different hydrolytic reaction, sharing mechanism with dehalogenation, or may have been involved in the

dehalogenation of naturally occurring halogenated compounds (Gribble, 2010; Janssen et al., 2005). The high abundance of naturally produced halogenated compounds in the environment makes the later proposition quite feasible. Genomic analysis of marine organisms expressing HLDs could provide valuable insights into the evolutionary origins of their biological function. Various alternative approaches can be used to uncover physiological function of enzymes: (i) targeted metabolomics, (ii) activity-based metabolomic profiling, (iii) gene knockouts, (iv) coexpression and transcriptome analysis, or (v) computational docking of metabolites to the structural models (Prosser, Larrouy-Maumus, & de Carvalho, 2014).

Members of the HLD-III subfamily are of special interest since they display dehalogenase activities in orders of magnitude lower than the members of the other two HLD subgroups. Moreover, a recent study identified  $\beta$ -lactone decarboxylase function in enzymes that share structural features with HLD-III subfamily and have only residual activity toward linear haloalkanes (Christenson et al., 2017). Testing of other members of this subfamily to different activities besides dehalogenation will shed a light on the other biological function of HLD-like enzymes.

Detailed mechanistic and kinetic analyses of individual HLDs are necessary for the understanding of the structural basis of dehalogenase catalytic mechanism and the investigation of enzyme evolution at a molecular level. An impressive amount of information has been collected from the analyses of four archetypal enzymes: DhaA, LinB, DhlA, and DbjA. Newly identified HLDs are often subjected to only a limited characterization without subsequent exploration of their unusual or interesting properties, mainly due to the high cost and time demands of experiments. Miniaturization of analytical methods together with the development of fast screening assays will significantly increase the efficiency of biochemical characterization and allow systematic probing of sequence space. A promising development in this direction is employing a microfluidics approach that has the potential to integrate alternative analytical tools. Moreover, a combination of high-throughput analytical tools with an automated platform for bioinformatics identification of novel HLDs in genomic databases (software tool EnzymeMiner under development) will provide an alternative approach for obtaining efficient and robust biocatalysts for practical applications.

HLDs found in marine organisms show interesting properties including high levels of activity toward a broad spectrum of substrates, diverse range of stability including the highest stability of all wild-type enzymes, and selective conversion of racemic mixtures of valuable synthons  $\alpha$ -bromoalkanes and

$\beta$ -bromoesters (Buryška et al., 2018; Chrast et al., 2018; Fortova et al., 2013). Biochemical characterization of marine HLDs clearly demonstrates a huge potential of the marine environment for the continued discovery of HLDs with new catalytic properties.

## ACKNOWLEDGMENTS

This work was supported by the Grant Agency of the Czech Republic (GA16-07965S), the National Sustainability Programme of the Czech Ministry of Education, Youth and Sports (LO1214, LQ1605), the research infrastructures (LM2015051, LM2015047, LM2015055), and the European Union project Raft4Biotech (720776). A.K. is the holder of Brno PhD Talent Scholarship and funded by the Brno City Municipality. The authors would like to express gratitude to all colleagues from Loschmidt Laboratories for their help during manuscript preparation.

## REFERENCES

- Abraham, W. R., Meyer, H., & Yakimov, M. (1998). Novel glycine containing glucolipids from the alkane using bacterium *Alcanivorax borkumensis*. *Biochimica et Biophysica Acta*, 1393(1), 57–62. [https://doi.org/10.1016/S0005-2760\(98\)00058-7](https://doi.org/10.1016/S0005-2760(98)00058-7).
- Agarwal, V., Miles, Z. D., Winter, J. M., Eustaquio, A. S., El Gamal, A. A., & Moore, B. S. (2017). Enzymatic halogenation and dehalogenation reactions: Pervasive and mechanistically diverse. *Chemical Reviews*, 117(8), 5619–5674. <https://doi.org/10.1021/acs.chemrev.6b00571>.
- Ahn, Y., Rhee, S. K., Fennell, D. E., Kerkhof, J., Hentschel, U., & Häggblom, M. M. (2003). Reductive dehalogenation of brominated phenolic compounds by microorganisms associated with the marine sponge *Aplysina aerophoba*. *Applied and Environmental Microbiology*, 69(7), 4159–4166. <https://doi.org/10.1128/AEM.69.7.4159>.
- Arbon, R. E., & Grimsrud, E. P. (1990). Selective detection of iodinated hydrocarbons by the electron capture detector with negative ion hydration and photodetachment. *Analytical Chemistry*, 62(17), 1762–1768. <https://doi.org/10.1021/ac00216a009>.
- Babkova, P., Sebestova, E., Brezovsky, J., Chaloupkova, R., & Damborsky, J. (2017). Ancestral haloalkane dehalogenases show robustness and unique substrate specificity. *Chembiochem*, 18(14), 1448–1456. <https://doi.org/10.1002/cbic.201700197>.
- Bednar, D., Beerens, K., Sebestova, E., Bendl, J., Khare, S., Chaloupkova, R., et al. (2015). FireProt:Energy- and evolution-based computational design of thermostable multiple-point mutants. *PLoS Computational Biology*, 11(11), e1004556. <https://doi.org/10.1371/journal.pcbi.1004556>.
- Bergmann, J. G., & Sanik, J. (1957). Determination of trace amounts of chlorine in naphtha. *Analytical Chemistry*, 29(2), 241–243. <https://doi.org/10.1021/ac60122a018>.
- Bidmanova, S., Chaloupkova, R., Damborsky, J., & Prokop, Z. (2010). Development of an enzymatic fiber-optic biosensor for detection of halogenated hydrocarbons. *Analytical and Bioanalytical Chemistry*, 398(5), 1891–1898. <https://doi.org/10.1007/s00216-010-4083-z>.
- Bidmanova, S., Damborsky, J., & Prokop, Z. (2013). Immobilization of haloalkane dehalogenase LinB from *Sphingobium japonicum* UT26 for biotechnological applications. *Journal of Biocatalysis & Biotransformation*, 2(1), 1–7. <https://doi.org/10.4172/2324-9099.1000106>.
- Bidmanova, S., Kotlanova, M., Rataj, T., Damborsky, J., Trtilek, M., & Prokop, Z. (2016). Fluorescence-based biosensor for monitoring of environmental pollutants: From



- concept to field application. *Biosensors & Bioelectronics*, 84, 97–105. <https://doi.org/10.1016/j.bios.2015.12.010>.
- Bloom, J. D., Labthavikul, S. T., Otey, C. R., & Arnold, F. H. (2006). Protein stability promotes evolvability. *Proceedings of the National Academy of Sciences of the United States of America*, 103(15), 5869–5874. <https://doi.org/10.1073/pnas.0510098103>.
- Bohac, M., Nagata, Y., Prokop, Z., Prokop, M., Monincova, M., Tsuda, M., et al. (2002). Halide-stabilizing residues of haloalkane dehalogenases studied by quantum mechanic calculations and site-directed mutagenesis. *Biochemistry*, 41(48), 14272–14280. <https://doi.org/10.1021/bi026427v>.
- Bommarius, A. S., & Paye, M. F. (2013). Stabilizing biocatalysts. *Chemical Society Reviews*, 42(15), 6534–6565. <https://doi.org/10.1039/c3cs60137d>.
- Bosma, T., Pikkemaat, M. G., Kingma, J., Dijk, J., & Janssen, D. B. (2003). Steady-state and pre-steady-state kinetic analysis of halopropane conversion by a *Rhodococcus* haloalkane dehalogenase. *Biochemistry*, 42(26), 8047–8053. <https://doi.org/10.1021/bi026907m>.
- Brezovsky, J., Babkova, P., Degtjarik, O., Fortova, A., Gora, A., Iermak, I., et al. (2016). Engineering a de novo transport tunnel. *ACS Catalysis*, 6(11), 7597–7610. <https://doi.org/10.1021/acscatal.6b02081>.
- Buryska, T., Babkova, P., Vavra, O., Damborsky, J., & Prokop, Z. (2018). A Haloalkane dehalogenase from a marine microbial consortium possessing exceptionally broad substrate specificity. *Applied and Environmental Microbiology*, 84(2), 1–13, e01684–17. <https://doi.org/10.1128/AEM.01684-17>.
- Buryska, T., Daniel, L., Kunka, A., Brezovsky, J., Damborsky, J., & Prokop, Z. (2016). Discovery of novel haloalkane dehalogenase inhibitors. *Applied and Environmental Microbiology*, 82(6), 1958–1965. <https://doi.org/10.1128/AEM.03916-15>.
- Cabrita, M. T., Vale, C., & Rauter, A. P. (2010). Halogenated compounds from marine algae. *Marine Drugs*, 8(8), 2301–2317. <https://doi.org/10.3390/md8082301>.
- Campbell, D. W., Müller, C., & Reardon, K. F. (2006). Development of a fiber optic enzymatic biosensor for 1,2-dichloroethane. *Biotechnology Letters*, 28(12), 883–887. <https://doi.org/10.1007/s10529-006-9014-x>.
- Chaloupkova, R., Prokop, Z., Sato, Y., Nagata, Y., & Damborsky, J. (2011). Stereoselectivity and conformational stability of haloalkane dehalogenase DbjA from *Bradyrhizobium japonicum* USDA110: The effect of pH and temperature. *FEBS Journal*, 278(15), 2728–2738. <https://doi.org/10.1111/j.1742-4658.2011.08203.x>.
- Chaloupkova, R., Prudnikova, T., Rezacova, P., Prokop, Z., Koudelakova, T., Daniel, L., et al. (2014). Structural and functional analysis of a novel haloalkane dehalogenase with two halide-binding sites. *Acta Crystallographica Section D: Biological Crystallography*, 70(7), 1884–1897. <https://doi.org/10.1107/S1399004714009018>.
- Chang, Z., Sitachitta, N., Rossi, J. V., Roberts, M. A., Flatt, P. M., Jia, J., et al. (2004). Biosynthetic pathway and gene cluster analysis of curacin A, an antitubulin natural product from the tropical marine cyanobacterium *Lyngbya majuscula*. *Journal of Natural Products*, 67(8), 1356–1367. <https://doi.org/10.1021/np0499261>.
- Chen, C. S., Fujimoto, Y., Girdaukas, G., & Sih, C. J. (1982). Quantitative analyses of biochemical kinetic resolutions of enantiomers. *Journal of the American Chemical Society*, 104(25), 7294–7299. <https://doi.org/10.1021/ja00389a064>.
- Chovancova, E., Kosinski, J., Bujnicki, J. M., & Damborsky, J. (2007). Phylogenetic analysis of haloalkane dehalogenases. *Proteins*, 67, 305–316. <https://doi.org/10.1002/prot>.
- Chrast, L., Tratsiak, K., Daniel, L., Sebestova, E., Prudnikova, T., Brezovsky, J., et al. (2018). Structural basis of paradoxically thermostable dehalogenase from psychrophilic bacterium. under review.
- Christenson, J. K., Robinson, S. L., Engel, T. A., Richman, J. E., Kim, A. N., & Wackett, L. P. (2017). OleB from bacterial hydrocarbon biosynthesis is a  $\beta$ -lactone decarboxylase sharing key features with haloalkane dehalogenases. *Biochemistry*, 56(40), 5278–5287. <https://doi.org/10.1021/acs.biochem.7b00667>.



- Clark, K., Karsch-Mizrachi, I., Lipman, D. J., Ostell, J., & Sayers, E. W. (2016). GenBank. *Nucleic Acids Research*, 44(D1), D67–D72. <https://doi.org/10.1093/nar/gkv1276>.
- Curragh, H., Flynn, O., Larkin, M. J., Stafford, T. M., Hamilton, J. T. G., & Harper, D. B. (1994). Haloalkane degradation and assimilation by *Rhodococcus rhodochrous* NCIMB 13064. *Microbiology*, 140, 1433–1442. <https://doi.org/10.1099/00221287-140-6-1433>.
- Damborsky, J., Chaloupkova, R., Pavlova, M., Chovancova, E., & Brezovsky, J. (2010). Structure–function relationships and engineering of haloalkane dehalogenases. In K. N. Timmis (Ed.), *Handbook of hydrocarbon and lipid microbiology* (pp. 1081–1098). Berlin: Springer. <https://doi.org/10.1007/978-3-540-77587-4>.
- Damborsky, J., Rorije, E., Jesenska, A., Nagata, Y., Klopman, G., & Peijnenburg, W. J. G. M. (2001). Structure–specificity relationships for haloalkane dehalogenases. *Environmental Toxicology and Chemistry*, 20(12), 2681–2689. <https://doi.org/10.1002/etc.5620201205>.
- Daniel, L., Buryška, T., Prokop, Z., Damborsky, J., & Brezovsky, J. (2014). Mechanism-based discovery of novel substrates of haloalkane dehalogenases using *in silico* screening. *Journal of Chemical Information and Modeling*, 55(1), 54–62. <https://doi.org/10.1021/ci500486y>.
- DeCastro, M. E., Rodríguez-Belmonte, E., & González-Siso, M. I. (2016). Metagenomics of thermophiles with a focus on discovery of novel thermozymes. *Frontiers in Microbiology*, 1–21. 7(SEP). <https://doi.org/10.3389/fmicb.2016.01521>.
- Deller, M. C., Kong, L., & Rupp, B. (2016). Protein stability: A crystallographer's perspective. *Acta Crystallographica Section F Structural Biology*, 72(2), 72–95. <https://doi.org/10.1107/S2053230X15024619>.
- Dörr, M., Fibinger, M. P. C., Last, D., Schmidt, S., Santos-Aberturas, J., Böttcher, D., et al. (2016). Fully automatized high-throughput enzyme library screening using a robotic platform. *Biotechnology and Bioengineering*, 113(7), 1421–1432. <https://doi.org/10.1002/bit.25925>.
- Drienovska, I., Chovancova, E., Koudelakova, T., Damborsky, J., & Chaloupkova, R. (2012). Biochemical characterization of a novel haloalkane dehalogenase from a cold-adapted bacterium. *Applied and Environmental Microbiology*, 78(14), 4995–4998. <https://doi.org/10.1128/AEM.00485-12>.
- Dvorak, P., Bidmanova, S., Damborsky, J., & Prokop, Z. (2014). Immobilized synthetic pathway for biodegradation of toxic recalcitrant pollutant 1,2,3-trichloropropane. *Environmental Science and Technology*, 48(12), 6859–6866. <https://doi.org/10.1021/es500396r>.
- Dvorak, P., Kurumbang, N. P., Bendl, J., Brezovsky, J., Prokop, Z., & Damborsky, J. (2014). Maximizing the efficiency of multienzyme process by stoichiometry optimization. *Chembiochem: A European Journal of Chemical Biology*, 15(13), 1891–1895. <https://doi.org/10.1002/cbic.201402265>.
- Engene, N., Rottacker, E. C., Kastovsky, J., Byrum, T., Choi, H., Ellisman, M. H., et al. (2012). *Moorea producens* gen. nov., sp. nov. and *Moorea bouillonii* comb. nov., tropical marine cyanobacteria rich in bioactive secondary metabolites. *International Journal of Systematic and Evolutionary Microbiology*, 62(5), 1171–1178. <https://doi.org/10.1099/ij.s.0.033761-0>.
- Fabritz, S., Maaß, F., Avrutina, O., Heiseler, T., Steinmann, B., & Kolmar, H. (2012). A sensitive method for rapid detection of alkyl halides and dehalogenase activity using a multistep enzyme assay. *AMB Express*, 2(51) <https://doi.org/10.1186/2191-0855-2-51>.
- Fasman, G. D. (Ed.), (1996). *Circular dichroism and the conformational analysis of biomolecules* (p. 738). Springer. <https://doi.org/10.1007/978-1-4757-2508-7>.
- Ferrer, M., Beloqui, A., Timmis, K. N., & Golyshein, P. N. (2008). Metagenomics for mining new genetic resources of microbial communities. *Journal of Molecular Microbiology and Biotechnology*, 16(1–2), 109–123. <https://doi.org/10.1159/000142898>.

- Fortova, A., Sebestova, E., Stepankova, V., Koudelakova, T., Palkova, L., Damborsky, J., et al. (2013). DspA from *Strongylocentrotus purpuratus*: The first biochemically characterized haloalkane dehalogenase of non-microbial origin. *Biochimie*, 95(11), 2091–2096. <https://doi.org/10.1016/j.biochi.2013.07.025>.
- Frasca, V. (2016). Using isothermal titration calorimetry techniques to quantify enzyme kinetics. *Industrial Biotechnology*, 12(4), 207–211. <https://doi.org/10.1089/ind.2016.29040.vfr>.
- Freyer, M. W., & Lewis, E. A. (2008). Isothermal titration calorimetry: Experimental design, data analysis, and probing macromolecule/ligand binding and kinetic interactions. *Methods in Cell Biology*, 84(7), 79–113. [https://doi.org/10.1016/S0091-679X\(07\)84004-0](https://doi.org/10.1016/S0091-679X(07)84004-0).
- Fung, H. K., Gadd, M. S., Drury, T. A., Cheung, S., Guss, J. M., Coleman, N. V., et al. (2015). Biochemical and biophysical characterisation of haloalkane dehalogenases DmrA and DmrB in *Mycobacterium* strain JS60 and their role in growth on haloalkanes. *Molecular Microbiology*, 97, 439–453. <https://doi.org/10.1111/mmi.13039>.
- Gasteiger, E., Gattiker, A., Hoogland, C., Ivanyi, I., Appel, R. D., & Bairoch, A. (2003). ExpASY: The proteomics server for in-depth protein knowledge and analysis. *Nucleic Acids Research*, 31(13), 3784–3788. <https://doi.org/10.1093/nar/gkg563>.
- Gehret, J. J., Gu, L., Geders, T. W., Brown, W. C., Gerwick, L., Gerwick, W. H., et al. (2012). Structure and activity of DmmA, a marine haloalkane dehalogenase. *Protein Science*, 21(2), 239–248. <https://doi.org/10.1002/pro.2009>.
- Glatz, Z., Marini, M. V., Wimmerova, M., Damborsky, J., & Nagata, Y. (2000). Determination of haloalkane dehalogenase activity by capillary zone electrophoresis. *Journal of Chromatography A*, 895(1–2), 219–225. [https://doi.org/10.1016/S0021-9673\(00\)00635-X](https://doi.org/10.1016/S0021-9673(00)00635-X).
- Glockner, F. O., Kube, M., Bauer, M., Teeling, H., Lombardot, T., Ludwig, W., et al. (2003). Complete genome sequence of the marine planctomycete *Pirellula* sp. strain 1. *Proceedings of the National Academy of Sciences of the United States of America*, 100(14), 8298–8303. <https://doi.org/10.1073/pnas.1431443100>.
- Gong, J. S., Lu, Z. M., Li, H., Zhou, Z. M., Shi, J. S., & Xu, Z. H. (2013). Metagenomic technology and genome mining: Emerging areas for exploring novel nitrilases. *Applied Microbiology and Biotechnology*, 97(15), 6603–6611. <https://doi.org/10.1007/s00253-013-4932-8>.
- Gray, K. A., Richardson, T. H., Kretz, K., Short, J. M., Bartnek, F., Knowles, R., et al. (2001). Rapid evolution of reversible denaturation and elevated melting temperature in a microbial haloalkane dehalogenase. *Advanced Synthesis & Catalysis*, 343(6–7), 607–617. [https://doi.org/10.1002/1615-4169\(200108\)343:6/7<607::AID-ADSC607>3.0.CO;2-M](https://doi.org/10.1002/1615-4169(200108)343:6/7<607::AID-ADSC607>3.0.CO;2-M).
- Gribble, G. W. (Ed.). (2010). *Naturally occurring organohalogen compounds—A comprehensive update* (p. 613). Vienna: Springer-Verlag. <https://doi.org/10.1007/978-3-211-99323-1>.
- Gribble, G. W. (2015). Biological activity of recently discovered halogenated marine natural products. *Marine Drugs*, 13(7), 4044–4136. <https://doi.org/10.3390/md13074044>.
- Guo, F., & Berglund, P. (2017). Transaminase biocatalysis: Optimization and application. *Green Chemistry*, 19(2), 333–360. <https://doi.org/10.1039/C6GC02328B>.
- Hansen, L. D., Transtrum, M. K., Quinn, C., & Demarse, N. (2016). Enzyme-catalyzed and binding reaction kinetics determined by titration calorimetry. *Biochimica et Biophysica Acta—General Subjects*, 1860(5), 957–966. <https://doi.org/10.1016/j.bbagen.2015.12.018>.
- Hårdeman, F., & Sjöling, S. (2007). Metagenomic approach for the isolation of a novel low-temperature-active lipase from uncultured bacteria of marine sediment. *FEMS Microbiology Ecology*, 59(2), 524–534. <https://doi.org/10.1111/j.1574-6941.2006.00206.x>.

- Hasan, K., Fortova, A., Koudelakova, T., Chaloupkova, R., Ishitsuka, M., Nagata, Y., et al. (2011). Biochemical characteristics of the novel haloalkane dehalogenase DatA, isolated from the plant pathogen *Agrobacterium tumefaciens* C58. *Applied and Environmental Microbiology*, 77(5), 1881–1884. <https://doi.org/10.1128/AEM.02109-10>.
- Hasan, K., Gora, A., Brezovsky, J., Chaloupkova, R., Moskalikova, H., Fortova, A., et al. (2013). The effect of a unique halide-stabilizing residue on the catalytic properties of haloalkane dehalogenase DatA from *Agrobacterium tumefaciens* C58. *The FEBS Journal*, 280(13), 3149–3159. <https://doi.org/10.1111/febs.12238>.
- Hesseler, M., Bogdanovic, X., Hidalgo, A., Berenguer, J., Palm, G. J., Hinrichs, W., et al. (2011). Cloning, functional expression, biochemical characterization, and structural analysis of a haloalkane dehalogenase from *Plesiocystis pacifica* SIR-1. *Applied Microbiology and Biotechnology*, 91(4), 1049–1060. <https://doi.org/10.1007/s00253-011-3328-x>.
- Holloway, P., Trevors, J. T., & Lee, H. (1998). A colorimetric assay for detecting haloalkane dehalogenase activity. *Journal of Microbiological Methods*, 32, 31–36.
- Hu, Y., Fu, C., Huang, Y., Yin, Y., Cheng, G., Lei, F., et al. (2010). Novel lipolytic genes from the microbial metagenomic library of the South China Sea marine sediment. *FEMS Microbiology Ecology*, 72(2), 228–237. <https://doi.org/10.1111/j.1574-6941.2010.00851.x>.
- Huang, J., Xin, Y., Cao, X., & Zhang, W. (2011). Phylogenetic diversity and characterization of 2-haloacid degrading bacteria from the marine sponge *Hymeniacidon perlevis*. *World Journal of Microbiology and Biotechnology*, 27(8), 1787–1794. <https://doi.org/10.1007/s11274-010-0636-8>.
- Ibarra-Molero, B., Naganathan, A. N., Sanchez-Ruiz, J. M., & Muñoz, V. (2015). Modern analysis of protein folding by differential scanning calorimetry. *Methods in Enzymology*, 567, 281–318. <https://doi.org/10.1016/bs.mie.2015.08.027>.
- Iizuka, T., Jojima, Y., Fudou, R., Hiraishi, A., Ahn, J. W., & Yamanaka, S. (2003). *Plesiocystis pacifica* gen. nov., sp. nov., a marine myxobacterium that contains dihydrogenated menaquinone, isolated from the Pacific coasts of Japan. *International Journal of Systematic and Evolutionary Microbiology*, 53(1), 189–195. <https://doi.org/10.1099/ijs.0.02418-0>.
- Iwasaki, I., Utsumi, S., & Ozawa, T. (1952). New colorimetric determination of chloride using mercuric thiocyanate and ferric ion. *Bulletin of the Chemical Society of Japan*, 25, 226–226. <https://doi.org/10.1246/bcsj.25.226>.
- Janssen, D. B. (2004). Evolving haloalkane dehalogenases. *Current Opinion in Chemical Biology*, 8(2), 150–159. <https://doi.org/10.1016/j.cbpa.2004.02.012>.
- Janssen, D. B., Dinkla, I. J. T., Poelarends, G. J., & Terpstra, P. (2005). Bacterial degradation of xenobiotic compounds: Evolution and distribution of novel enzyme activities. *Environmental Microbiology*, 7(12), 1868–1882. <https://doi.org/10.1111/j.1462-2920.2005.00966.x>.
- Janssen, D. B., Gerritse, J., Brackman, J., Kalk, C., Jager, D., & Witholt, B. (1988). Purification and characterization of a bacterial dehalogenase with activity toward halogenated alkanes, alcohols and ethers. *European Journal of Biochemistry*, 171(1–2), 67–72. <http://www.ncbi.nlm.nih.gov/pubmed/3338472>.
- Jesenska, A., Bartos, M., Czernekova, V., Rychlik, I., Pavlik, I., & Damborsky, J. (2002). Cloning and expression of the haloalkane dehalogenase gene dhmA from *Mycobacterium avium* N85 and preliminary characterization of DhmA. *Applied and Environmental Microbiology*, 68(8), 3724–3730. <https://doi.org/10.1128/AEM.68.8.3724-3730.2002>.
- Jesenska, A., Monincova, M., Koudelakova, T., Hasan, K., Chaloupkova, R., Prokop, Z., et al. (2009). Biochemical characterization of haloalkane dehalogenases DrbA and DmbC, representatives of a novel subfamily. *Applied and Environmental Microbiology*, 75(15), 5157–5160. <https://doi.org/10.1128/AEM.00199-09>.
- Jesenska, A., Pavlova, M., Strouhal, M., Chaloupkova, R., Tesinska, I., Monincova, M., et al. (2005). Cloning, biochemical properties, and distribution of mycobacterial haloalkane dehalogenases. *Applied and Environmental Microbiology*, 71(11), 6736–6745. <https://doi.org/10.1128/AEM.71.11.6736-6745.2005>.

- Jesenska, A., Sedlacek, I., & Damborsky, J. (2000). Dehalogenation of haloalkanes by *Mycobacterium tuberculosis* H37Rv and other mycobacteria these include: Dehalogenation of haloalkanes by mycobacterium tuberculosis H37Rv and other mycobacteria. *Applied and Environmental Microbiology*, 66(1), 219–222. <https://doi.org/10.1128/AEM.66.1.219-222.2000>. Updated.
- Kasai, Y., Kishira, H., Sasaki, T., Syutsubo, K., Watanabe, K., & Harayama, S. (2002). Predominant growth of *Alcanivorax* strains in oil-contaminated and nutrient-supplemented sea water. *Environmental Microbiology*, 4(3), 141–147. <https://doi.org/10.1046/j.1462-2920.2002.00275.x>.
- Kelly, S., & Price, N. (2000). The use of circular dichroism in the investigation of protein structure and function. *Current Protein & Peptide Science*, 1(4), 349–384. <https://doi.org/10.2174/1389203003381315>.
- Kennedy, J., Marchesi, J. R., & Dobson, A. D. (2008). Marine metagenomics: Strategies for the discovery of novel enzymes with biotechnological applications from marine environments. *Microbial Cell Factories*, 7(1), 27. <https://doi.org/10.1186/1475-2859-7-27>.
- Keuning, S., Janssen, D. B., & Witholt, B. (1985). Purification and characterization of hydrolytic haloalkane dehalogenase from *Xanthobacter autotrophicus* GJ10. *Journal of Bacteriology*, 163(2), 635–639.
- Kokkonen, P., Koudelakova, T., Chaloupkova, R., Prokop, Z., & Damborsky, J. (2017). Structure–function relationships and engineering of haloalkane dehalogenases. In F. Rojo (Ed.), *Aerobic utilization of hydrocarbons, oils and lipids* (pp. 1–21). Springer. <https://doi.org/10.1007/978-3-319-39782-5>.
- König, G. M., & Wright, A. D. (1997). Laurencia rigida: Chemical investigations of its anti-fouling dichloromethane extract. *Journal of Natural Products*, 60(10), 967–970. <https://doi.org/10.1021/np970181r>.
- Koopmeiners, J., Halmschlag, B., Schallmey, M., & Schallmey, A. (2016). Biochemical and biocatalytic characterization of 17 novel haloalcohol dehalogenases. *Applied Microbiology and Biotechnology*, 100(17), 7517–7527. <https://doi.org/10.1007/s00253-016-7493-9>.
- Kotik, M., Vanacek, P., Kunka, A., Prokop, Z., & Damborsky, J. (2017). Metagenome-derived haloalkane dehalogenases with novel catalytic properties. *Applied Microbiology and Biotechnology*, 101(16), 6385–6397. <https://doi.org/10.1007/s00253-017-8393-3>.
- Koudelakova, T., Bidmanova, S., Dvorak, P., Pavelka, A., Chaloupkova, R., Prokop, Z., et al. (2013). Haloalkane dehalogenases: Biotechnological applications. *Biotechnology Journal*, 8(1), 32–45. <https://doi.org/10.1002/biot.201100486>.
- Koudelakova, T., Chaloupkova, R., Brezovsky, J., Prokop, Z., Sebestova, E., Hesseler, M., et al. (2013). Engineering enzyme stability and resistance to an organic cosolvent by modification of residues in the access tunnel. *Angewandte Chemie—International Edition*, 52(7), 1959–1963. <https://doi.org/10.1002/anie.201206708>.
- Koudelakova, T., Chovancova, E., Brezovsky, J., Monincova, M., Fortova, A., Jarkovsky, J., et al. (2011). Substrate specificity of haloalkane dehalogenases. *The Biochemical Journal*, 435(2), 345–354. <https://doi.org/10.1042/BJ20101405>.
- Kulakov, L. A., Poelarends, G. J., Janssen, D. B., & Larkin, M. J. (1999). Characterization of IS 2112, a new insertion sequence from *Rhodococcus*, and its relationship with mobile elements belonging to the IS 110 family. *Microbiology*, 145(Pt 3), 561–568. <https://doi.org/10.1099/13500872-145-3-561>.
- Kulakova, A. N., Larkin, M. J., & Kulakov, L. A. (1997). The plasmid-located haloalkane dehalogenase gene from *Rhodococcus rhodochrous* NCIMB 13064. *Microbiology*, 143(Pt 1), 109–115. <https://doi.org/10.1099/00221287-143-1-109>.
- Lane, A. L., Nyadong, L., Galhena, A. S., Shearer, T. L., Stout, E. P., Parry, R. M., et al. (2009). Desorption electrospray ionization mass spectrometry reveals surface-mediated antifungal chemical defense of a tropical seaweed. *Proceedings of the National Academy of*

- Sciences of the United States of America*, 106(18), 7314–7319. <https://doi.org/10.1073/pnas.0812020106>.
- Lee, H. K., Chun, J., Moon, E. Y., Ko, S., Lee, D., Lee, H. S., et al. (2001). *Hahella chejuensis* gen. nov., sp. nov., an extracellular-polysaccharide-producing marine bacterium. *International Journal of Systematic and Evolutionary Microbiology*, 51(Pt 2), 661–666.
- Li, A., & Shao, Z. (2014). Biochemical characterization of a haloalkane dehalogenase DadB from *Alcanivorax dieselolei* B-5. *PLoS one*, 9(2), e89144. <https://doi.org/10.1371/journal.pone.0089144>.
- Liang, B., Jiang, J., Zhang, J., Zhao, Y., & Li, S. (2012). Horizontal transfer of dehalogenase genes involved in the catalysis of chlorinated compounds: Evidence and ecological role. *Critical Reviews in Microbiology*, 38(2), 1–16. <https://doi.org/10.3109/1040841X.2011.618114>.
- Liskova, V., Bednar, D., Prudnikova, T., Rezacova, P., Koudelakova, T., Sebestova, E., et al. (2015). Balancing the stability–activity trade-off by fine-tuning dehalogenase access tunnels. *ChemCatChem*, 7(4), 648–659. <https://doi.org/10.1002/cctc.201402792>.
- Liskova, V., Stepankova, V., Bednar, D., Brezovsky, J., Prokop, Z., Chaloupkova, R., et al. (2017). Different structural origins of the enantioselectivity of haloalkane dehalogenases toward linear  $\beta$ -haloalkanes: Open-solvated versus occluded-desolvated active sites. *Angewandte Chemie—International Edition*, 56(17), 4719–4723. <https://doi.org/10.1002/anie.201611193>.
- Liu, C., & Shao, Z. (2005). *Alcanivorax dieselolei* sp. nov., a novel alkane-degrading bacterium isolated from sea water and deep-sea sediment. *International Journal of Systematic and Evolutionary Microbiology*, 55(3), 1181–1186. <https://doi.org/10.1099/ijs.0.63443-0>.
- Liu, C., Wang, W., Wu, Y., Zhou, Z., Lai, Q., & Shao, Z. (2011). Multiple alkane hydroxylase systems in a marine alkane degrader, *Alcanivorax dieselolei* B-5. *Environmental Microbiology*, 13(5), 1168–1178. <https://doi.org/10.1111/j.1462-2920.2010.02416.x>.
- Loos, M. A. (1975). Indicator media for microorganisms degrading chlorinated pesticides. *Canadian Journal of Microbiology*, 21(1), 104–107. <https://doi.org/10.1139/m75-016>.
- Marchesi, J. R. (2003). A microplate fluorimetric assay for measuring dehalogenase activity. *Journal of Microbiological Methods*, 55(1), 325–329. [https://doi.org/10.1016/S0167-7012\(03\)00132-5](https://doi.org/10.1016/S0167-7012(03)00132-5).
- Marvanova, S., Nagata, Y., Wimmerova, M., Sykorova, J., Hynkova, K., & Damborsky, J. (2001). Biochemical characterization of broad-specificity enzymes using multivariate experimental design and a colorimetric microplate assay: Characterization of the haloalkane dehalogenase mutants. *Journal of Microbiological Methods*, 44, 149–157. [https://doi.org/10.1016/S0167-7012\(00\)00250-5](https://doi.org/10.1016/S0167-7012(00)00250-5).
- Mattes, T. E., Alexander, A. K., Richardson, P. M., Munk, A. C., Han, C. S., Stothard, P., et al. (2008). The genome of *Polaromonas* sp. strain JS666: Insights into the evolution of a hydrocarbon- and xenobiotic-degrading bacterium, and features of relevance to biotechnology. *Applied and Environmental Microbiology*, 74(20), 6405–6416. <https://doi.org/10.1128/AEM.00197-08>.
- Mazurenko, S., Kunka, A., Beerens, K., Johnson, C. M., Damborsky, J., & Prokop, Z. (2017). Exploration of protein unfolding by modelling calorimetry data from reheating. *Scientific Reports*, 7(1), 16321. <https://doi.org/10.1038/s41598-017-16360-y>.
- Mazurenko, S., Stourac, J., Kunka, A., Nedeljkovic, S., Bednar, D., Prokop, Z., et al. (2018). CalFitter: Web server for protein thermal denaturation data analysis. *Nucleic Acid Research*, 1–7 (accepted manuscript).
- Monincova, M., Prokop, Z., Vevodova, J., Nagata, Y., & Damborsky, J. (2007). Weak activity of haloalkane dehalogenase LinB with 1,2,3-trichloropropane revealed by X-ray crystallography and microcalorimetry. *Applied and Environmental Microbiology*, 73(6), 2005–2008. <https://doi.org/10.1128/AEM.02416-06>.

- Nagata, Y., Miyauchi, K., & Takagi, M. (1999). Complete analysis of genes and enzymes for gamma-hexachlorocyclohexane degradation in *Sphingomonas paucimobilis* UT26. *Journal of Industrial Microbiology and Biotechnology*, 23(4–5), 380–390. <https://doi.org/10.1038/sj.jim.2900736>.
- Nagata, Y., Nariya, T., Ohtomo, R., Fukuda, M., Yano, K., & Takagi, M. (1993). Cloning and sequencing of a dehalogenase gene encoding an enzyme with hydrolase gamma-hexachlorocyclohexane in cloning and sequencing of a dehalogenase gene encoding an enzyme with hydrolase activity involved in the degradation of  $\gamma$ -hexachlorocyclohexane. *Journal of Bacteriology*, 175(20), 6403–6410. <https://doi.org/10.1128/jb.175.20.6403-6410.1993>.
- Nagata, Y., Ohtsubo, Y., & Tsuda, M. (2015). Properties and biotechnological applications of natural and engineered haloalkane dehalogenases. *Applied Microbiology and Biotechnology*, 99(23), 9865–9881. <https://doi.org/10.1007/s00253-015-6954-x>.
- Nagata, Y., Prokop, Z., Marvanova, S., Sykorova, J., Monincova, M., Tsuda, M., et al. (2003). Reconstruction of mycobacterial dehalogenase Rv2579 by cumulative mutagenesis of haloalkane dehalogenase LinB. *Applied and Environmental Microbiology*, 69(4), 2349–2355. <https://doi.org/10.1128/AEM.69.4.2349-2355.2003>.
- Nagata, Y., Prokop, Z., Sato, Y., Jerabek, P., Kumar, A., Ohtsubo, Y., et al. (2005). Degradation of  $\beta$ -hexachlorocyclohexane by haloalkane dehalogenase LinB from *Sphingomonas paucimobilis* UT26. *Applied and Environmental Microbiology*, 71(4), 2183–2185. <https://doi.org/10.1128/AEM.71.4.2183>.
- Nakamura, T., Zamocky, M., Zdrahal, Z., Chaloupkova, R., Monincova, M., Prokop, Z., et al. (2006). Expression of glycosylated haloalkane dehalogenase LinB in *Pichia pastoris*. *Protein Expression and Purification*, 46(1), 85–91. <https://doi.org/10.1016/j.pep.2005.08.022>.
- Nardini, M., & Dijkstra, B. W. (1999).  $\alpha/\beta$  hydrolase fold enzymes: The family keeps growing. *Current Opinion in Structural Biology*, 9(6), 732–737. [https://doi.org/10.1016/S0959-440X\(99\)00037-8](https://doi.org/10.1016/S0959-440X(99)00037-8).
- Nguyen, L. A., He, H., & Pham-Huy, C. (2006). Chiral drugs: An overview. *International Journal of Biomedical Science: IJBS*, 2(2), 85–100.
- Novak, H. R., Sayer, C., Isupov, M. N., Gotz, D., Spragg, A. M., & Littlechild, J. A. (2014). Biochemical and structural characterisation of a haloalkane dehalogenase from a marine *Rhodobacteraceae*. *FEBS Letters*, 588(9), 1616–1622. <https://doi.org/10.1016/j.febslet.2014.02.056>.
- Novak, H. R., Sayer, C., Isupov, M. N., Paszkiewicz, K., Gotz, D., Mearns Spragg, A., et al. (2013). Marine *Rhodobacteraceae* I-haloacid dehalogenase contains a novel His/Glu dyad that could activate the catalytic water. *The FEBS Journal*, 280(7), 1664–1680. <https://doi.org/10.1111/febs.12177>.
- Oakley, A. J., Prokop, Z., Bohac, M., Kmunicek, J., Jedlicka, T., Monincova, M., et al. (2002). Exploring the structure and activity of haloalkane dehalogenase from *Sphingomonas paucimobilis* UT26: Evidence for product- and water-mediated inhibition. *Biochemistry*, 41(15), 4847–4855. <https://doi.org/10.1021/bi015734i>.
- Ohana, R. F., Encell, L. P., Zhao, K., Simpson, D., Slater, M. R., Urh, M., et al. (2009). HaloTag7: A genetically engineered tag that enhances bacterial expression of soluble proteins and improves protein purification. *Protein Expression and Purification*, 68(1), 110–120. <https://doi.org/10.1016/j.pep.2009.05.010>.
- Ollis, D. L., Cheah, E., Cygler, M., Dijkstra, B., Frolow, F., Franken, S. M., et al. (1992). The  $\alpha/\beta$  hydrolase fold. *Protein Engineering, Design and Selection*, 5(3), 197–211. <https://doi.org/10.1093/protein/5.3.197>.
- Pavlova, M., Klvana, M., Prokop, Z., Chaloupkova, R., Banas, P., Otyepka, M., et al. (2009). Redesigning dehalogenase access tunnels as a strategy for degrading an anthropogenic substrate. *Nature Chemical Biology*, 5(10), 727–733. <https://doi.org/10.1038/nchembio.205>.



- Pieters, R. J., Lutje Spelberg, J. H., Kellogg, R. M., & Janssen, D. B. (2001). The enantioselectivity of haloalkane dehalogenases. *Tetrahedron Letters*, 42(3), 469–471. [https://doi.org/10.1016/S0040-4039\(00\)01947-X](https://doi.org/10.1016/S0040-4039(00)01947-X).
- Pikkemaat, M. G., & Janssen, D. B. (2002). Generating segmental mutations in haloalkane dehalogenase: A novel part in the directed evolution toolbox. *Nucleic Acids Research*, 30(8), E35. <https://doi.org/10.1093/nar/30.8.e35>.
- Poelarends, G. J., Kulakov, L. A., Larkin, M. J., Van Hylckama Vlieg, J. E. T., & Janssen, D. B. (2000). Roles of horizontal gene transfer and gene integration in evolution of 1,3-dichloropropene- and 1,2-dibromoethane-degradative pathways. *Journal of Bacteriology*, 182(8), 2191–2199. <https://doi.org/10.1128/JB.182.8.2191-2199.2000>.
- Poelarends, G. J., Zandstra, M., Bosma, T., Kulakov, L. A., Larkin, M. J., Marchesi, J. R., et al. (2000). Haloalkane-utilizing rhodococcus strains isolated from geographically distinct locations possess a highly conserved gene cluster encoding haloalkane catabolism. *Journal of Bacteriology*, 182(10), 2725–2731. <https://doi.org/10.1128/JB.182.10.2725-2731.2000>.
- Pollard, D. J., & Woodley, J. M. (2007). Biocatalysis for pharmaceutical intermediates: The future is now. *Trends in Biotechnology*, 25(2), 66–73. <https://doi.org/10.1016/j.tibtech.2006.12.005>.
- Privalov, G. P., & Privalov, P. L. (2000). Problems and prospects in microcalorimetry of biological macromolecules. *Methods in Enzymology*, 323, 31–62. [https://doi.org/10.1016/S0076-6879\(00\)23360-0](https://doi.org/10.1016/S0076-6879(00)23360-0).
- Privalov, P. L., & Dragan, A. I. (2007). Microcalorimetry of biological macromolecules. *Biophysical Chemistry*, 126(1–3), 16–24. <https://doi.org/10.1016/j.bpc.2006.05.004>.
- Prokop, Z., Monincova, M., Chaloupkova, R., Klvana, M., Nagata, Y., Janssen, D. B., et al. (2003). Catalytic mechanism of the haloalkane dehalogenase LinB from *Sphingomonas paucimobilis* UT26. *Journal of Biological Chemistry*, 278(46), 45094–45100. <https://doi.org/10.1074/jbc.M307056200>.
- Prokop, Z., Oplustil, F., DeFrank, J., & Damborsky, J. (2006). Enzymes fight chemical weapons. *Biotechnology Journal*, 1(12), 1370–1380. <https://doi.org/10.1002/biot.200600166>.
- Prokop, Z., Sato, Y., Brezovsky, J., Mozga, T., Chaloupkova, R., Koudelakova, T., et al. (2010). Enantioselectivity of haloalkane dehalogenases and its modulation by surface loop engineering. *Angewandte Chemie International Edition*, 49(35), 6111–6115. <https://doi.org/10.1002/anie.201001753>.
- Prosser, G. A., Larrouy-Maumus, G., & de Carvalho, L. P. S. (2014). Metabolomic strategies for the identification of new enzyme functions and metabolic pathways. *EMBO Reports*, 15(6), 657–669. <https://doi.org/10.15252/embr.201338283>.
- Qiu, L. H., Li, C. X., Sun, J., Wang, Z., Ye, Q., & Xu, J. H. (2011). Thermostable bacterial endoglucanases mined from Swiss-Prot database. *Applied Biochemistry and Biotechnology*, 165(7–8), 1473–1484. <https://doi.org/10.1007/s12010-011-9368-y>.
- Sato, Y., Monincova, M., Chaloupkova, R., Prokop, Z., Ohtsubo, Y., Minamisawa, K., et al. (2005). Two rizobial strains, *Mesorhizobium loti* MAFF303099 and *Bradyrhizobium japonicum* USDA110, encode haloalkane dehalogenases with novel structures and substrate specificities. *Applied and Environmental Microbiology*, 71(8), 4372–4379. <https://doi.org/10.1128/AEM.71.8.4372-4379.2005>.
- Schallmeyer, M., Koopmeiners, J., Wells, E., Wardenga, R., & Schallmeyer, A. (2014). Expanding the halohydrin dehalogenase enzyme family: Identification of novel enzymes by database mining. *Applied and Environmental Microbiology*, 80(23), 7303–7315. <https://doi.org/10.1128/AEM.01985-14>.
- Schanstra, J. P., Kingma, J., & Janssen, D. B. (1996). Specificity and kinetics of haloalkane dehalogenase. *The Journal of Biological Chemistry*, 271(25), 14747–14753. Retrieved from <http://www.ncbi.nlm.nih.gov/pubmed/8662955>.

- Schindler, J. F., Naranjo, P. A., Honabberger, D. A., Chang, C. H., Brainard, J. R., Vanderberg, L. A., et al. (1999). Haloalkane dehalogenases: Steady-state kinetics and halide inhibition. *Biochemistry*, 38(18), 5772–5778. <https://doi.org/10.1021/bi982853y>.
- Schmid, A., Dordick, J. S., Hauer, B., Kiener, A., Wubbolts, M., & Witholt, B. (2001). Industrial biocatalysis today and tomorrow. *Nature*, 409(6817), 258–268. <https://doi.org/10.1038/35051736>.
- Sharma, P., Jindal, S., Bala, K., Kumari, K., Niharika, N., Kaur, J., et al. (2014). Functional screening of enzymes and bacteria for the dechlorination of hexachlorocyclohexane by a high-throughput colorimetric assay. *Biodegradation*, 25, 179–187. <https://doi.org/10.1007/s10532-013-9650-5>.
- Sneed, J. M., Sharp, K. H., Ritchie, K. B., & Paul, V. J. (2014). The chemical cue tetrabromopyrrole from a biofilm bacterium induces settlement of multiple Caribbean corals. *Proceedings of the Biological Sciences*, 281(1786). <https://doi.org/10.1098/rspb.2013.3086>.
- Stepankova, V., Damborsky, J., & Chaloupkova, R. (2013). Organic co-solvents affect activity, stability and enantioselectivity of haloalkane dehalogenases. *Biotechnology Journal*, 8(6), 719–729. <https://doi.org/10.1002/biot.201200378>.
- Stepankova, V., Khabiri, M., Brezovsky, J., Pavelka, A., Sykora, J., Amaro, M., et al. (2013). Expansion of access tunnels and active-site cavities influence activity of haloalkane dehalogenases in organic cosolvents. *Chembiochem: A European Journal of Chemical Biology*, 14(7), 890–897. <https://doi.org/10.1002/cbic.201200733>.
- Stepankova, V., Vanacek, P., Damborsky, J., & Chaloupkova, R. (2014). Comparison of catalysis by haloalkane dehalogenases in aqueous solutions of deep eutectic and organic solvents. *Green Chemistry*, 16(5), 2754–2761. <https://doi.org/10.1039/C4GC00117F>.
- Stucki, G., & Thüer, M. (1995). Experiences of a large-scale application of 1,2-dichloroethane degrading microorganisms for groundwater treatment. *Environmental Science and Technology*, 29(9), 2339–2345. <https://doi.org/10.1021/es00009a028>.
- Sykora, J., Brezovsky, J., Koudelakova, T., Lahoda, M., Fortova, A., Chernovets, T., et al. (2014). Dynamics and hydration explain failed functional transformation in dehalogenase design. *Nature Chemical Biology*, 10(6), 428–430. <https://doi.org/10.1038/nchembio.1502>.
- Tang, L., Li, Y., & Wang, X. (2010). A high-throughput colorimetric assay for screening haloalcohol dehalogenase saturation mutagenesis libraries. *Journal of Biotechnology*, 147(3–4), 164–168. <https://doi.org/10.1016/j.jbiotec.2010.04.002>.
- Todd, M. J., & Gomez, J. (2001). Enzyme kinetics determined using calorimetry: A general assay for enzyme activity? *Analytical Biochemistry*, 296(2), 179–187. <https://doi.org/10.1006/abio.2001.5218>.
- Tratsiak, K., Degtjarik, O., Drienovska, I., Chrast, L., Rezacova, P., Kutý, M., et al. (2013). Crystallographic analysis of new psychrophilic haloalkane dehalogenases: DpcA from *Psychrobacter cryohalolentis* K5 and DmxA from *Marinobacter* sp. ELB17. *Acta Crystallographica Section F: Structural Biology and Crystallization Communications*, 69(6), 683–686. <https://doi.org/10.1107/S1744309113012979>.
- Vanacek, P., Sebestova, E., Babkova, P., Bidmanova, S., Daniel, L., Dvorak, P., et al. (2018). Exploration of enzyme diversity by integrating bioinformatics with expression analysis and biochemical characterization. *ACS Catalysis*, 8(3), 2402–2412. <https://doi.org/10.1021/acscatal.7b03523>.
- Van Pee, K. H. (2001). Microbial biosynthesis of halometabolites. *Archives of Microbiology*, 175(4), 250–258. <https://doi.org/10.1007/s002030100263>.
- Van Pee, K. H., & Unversucht, S. (2003). Biological dehalogenation and halogenation reactions. *Chemosphere*, 52(2), 299–312. [https://doi.org/10.1016/S0045-6535\(03\)00204-2](https://doi.org/10.1016/S0045-6535(03)00204-2).
- Wang, W., & Shao, Z. (2014). The long-chain alkane metabolism network of *Alcanivorax dieselolei*. *Nature Communications*, 5, 5755. <https://doi.org/10.1038/ncomms6755>.



- Westerbeek, A., Szymański, W., Wijma, H. J., Marrink, S. J., Feringa, B. L., & Janssen, D. B. (2011). Kinetic resolution of  $\alpha$ -bromoamides: Experimental and theoretical investigation of highly enantioselective reactions catalyzed by haloalkane dehalogenases. *Advanced Synthesis and Catalysis*, 353(6), 931–944. <https://doi.org/10.1002/adsc.201000726>.
- Yakimov, M. M., Golyshin, P. N., Lang, S., Moore, E. R. B., Abraham, W., Lunsdorf, H., et al. (1998). *Alcanivorax borkumensis* gen. nov., sp. nov. a new, hydrocarbon-degrading and surfactant-producing marine bacterium. *International Journal of Systematic Bacteriology*, 48, 339–348. <https://doi.org/10.1099/00207713-48-2-339>.
- Zall, D. M., Fisher, D., & Garner, M. Q. (1956). Photometric determination of chlorides in water. *Analytical Chemistry*, 28, 1665–1668. <https://doi.org/10.1021/ac60119a009>.
- Zhao, H. (2003). A pH-indicator-based screen for hydrolytic haloalkane dehalogenase. In F. H. Arnold & G. Georgiou (Eds.), *Methods in molecular biology: Vol. 230. Directed enzyme evolution*. Humana Press. <https://doi.org/10.1385/1-59259-396-8:213>.